Modulation instability, periodic anomalous wave recurrence, and blow up in the Ablowitz–Ladik lattices

OPEN ACCESS
IOP Publishing
Journal of Physics A: Mathematical and Theoretical
J. Phys. A: Math. Theor. **57** (2024) 015202 (28pp)
https://doi.org/10.1088/1751-8121/ad0ce3

Modulation instability, periodic anomalous wave recurrence, and blow up in the Ablowitz–Ladik lattices

F Coppini[1,2,*] **and P M Santini**[1]

[1] Dipartimento di Fisica, Università di Roma 'La Sapienza', and Istituto Nazionale di Fisica Nucleare (INFN), Sezione di Roma, Piazz.le Aldo Moro 2, I-00185 Roma, Italy
[2] Department of Mathematics, Physics and Electrical Engineering, Northumbria University Newcastle, Newcastle upon Tyne NE1 8ST, United Kingdom

E-mail: francesco.coppini@uniroma1.it and francesco.coppini@roma1.infn.it

Received 22 June 2023; revised 1 October 2023
Accepted for publication 15 November 2023
Published 5 December 2023

Abstract

The Ablowitz–Ladik equations, hereafter called AL_+ and AL_-, are distinguished integrable discretizations of respectively the focusing and defocusing nonlinear Schrödinger (NLS) equations. In this paper we first study the modulation instability of the homogeneous background solutions of $AL_\pm$ in the periodic setting, showing in particular that the background solution of AL_- is unstable under a monochromatic perturbation of any wave number if the amplitude of the background is greater than 1, unlike its continuous limit, the defocusing NLS. Then we use Darboux transformations to construct the exact periodic solutions of $AL_\pm$ describing such instabilities, in the case of one and two unstable modes, and we show that the solutions of AL_- are always singular on curves of spacetime, if they live on a background of sufficiently large amplitude, and we construct a different continuous limit describing this regime: a NLS equation with a nonlinear and weak dispersion. At last, using matched asymptotic expansion techniques, we describe in terms of elementary functions how a generic periodic perturbation of the background solution (i) evolves according to AL_+ into a recurrence of the above exact solutions, in the case of one and two unstable modes, and (ii) evolves according to AL_- into a singularity in finite time if the amplitude of the background is greater than

* Author to whom any correspondence should be addressed.

1. The quantitative agreement between the analytic formulas of this paper and numerical experiments is perfect.

Keywords: Ablowitz–Ladik lattice, cauchy problem, solitons, modulation instability

1. Introduction

The Ablowitz–Ladik (AL) equations [2, 3]:

$$\begin{aligned} &i\dot{u}_n + u_{n+1} + u_{n-1} - 2u_n + \eta|u_n|^2(u_{n-1}+u_{n+1}) = 0, \quad \eta = \pm 1, \\ &u_n = u(n,t) \in \mathbb{C}, \quad \dot{u}_n = \tfrac{du_n(t)}{dt}, \quad n \in \mathbb{Z}, \quad t \in \mathbb{R}, \end{aligned} \tag{1}$$

are distinguished examples of integrable nonlinear differential-difference equations reducing, in the natural continuous limit

$$u_n(t) = ih\, v(\xi,\tau), \quad hn = \xi, \quad \tau = h^2 t, \quad h \to 0, \tag{2}$$

to the celebrated integrable [79] nonlinear Schrödinger (NLS) equations

$$\begin{aligned} &iv_\tau + v_{\xi\xi} + 2\eta|v|^2 v = 0, \ \eta = \pm 1, \\ &v(\xi,\tau) \in \mathbb{C}, \quad v_\tau = \tfrac{\partial v}{\partial \tau}, \quad v_{\xi\xi} = \tfrac{\partial^2 v}{\partial \xi^2}, \quad \xi,\tau \in \mathbb{R}, \end{aligned} \tag{3}$$

where h is the lattice spacing. The two cases $\eta = \pm 1$ in (3) distinguish between the very different focusing ($\eta = 1$) and defocusing ($\eta = -1$) NLS regimes.

The AL equation (1) characterize [38] the quantum correlation function of the XY-model of spins [48]. If $\eta = 1$, it is relevant in the study of anharmonic lattices [71]; it is gauge equivalent to an integrable discretization of the Heisenberg spin chain [37], and appears in the description of a lossless nonlinear electric lattice ($\eta = 1$) [51]. At last, if $\eta = 1$, the AL hierarchy describes the integrable motions of a discrete curve on the sphere [23].

The well-known Lax pair of equation (1) reads [2, 3]

$$\begin{aligned} &\vec{\psi}_{n+1}(t,\lambda) = L_n(t,\lambda)\vec{\psi}_n(t,\lambda), \quad \vec{\psi}_{n_t}(t,\lambda) = A_n(t,\lambda)\vec{\psi}_n(t,\lambda), \\ &L_n(t,\lambda) = \begin{pmatrix} \lambda & u_n(t) \\ -\eta\overline{u}_n(t) & \frac{1}{\lambda} \end{pmatrix}, \\ &A_n(t,\lambda) = i\begin{pmatrix} \lambda^2 - 1 + \eta u_n \overline{u}_{n-1} & \lambda u_n - \frac{u_{n-1}}{\lambda} \\ \eta\frac{\overline{u}_n}{\lambda} - \eta\lambda\overline{u}_{n-1} & 1 - \frac{1}{\lambda^2} - \eta\overline{u}_n u_{n-1} \end{pmatrix}, \end{aligned} \tag{4}$$

where $\bar{f}$ is the complex conjugate of f, and the matrices L_n and A_n of the Lax pair (4) possess the two symmetry

$$\begin{aligned} &L_n(\lambda) = P_\eta \overline{L_n\left(\tfrac{1}{\bar{\lambda}}\right)} P_\eta^\dagger = -\sigma_3 L_n(-\lambda)\,\sigma_3, \\ &A_n(\lambda) = P_\eta \overline{A_n\left(\tfrac{1}{\bar{\lambda}}\right)} P_\eta^\dagger = \sigma_3 A_n(-\lambda)\,\sigma_3, \end{aligned} \tag{5}$$

where

$$\sigma_3 = \begin{pmatrix} 1 & 0 \\ 0 & -1 \end{pmatrix}, \quad P_\eta = \begin{pmatrix} 0 & -\eta \\ 1 & 0 \end{pmatrix} \tag{6}$$

implying that, if $\vec{\psi}_n(\lambda,t) = (\psi_{1n}(\lambda,t), \psi_{2n}(\lambda,t))^T$ is solution of (4), then

$$\check{\vec{\psi}}_n(\lambda,t)=\begin{pmatrix} -\eta\overline{\psi_{2n}\left(\frac{1}{\bar\lambda},t\right)} \\ \overline{\psi_{1n}\left(\frac{1}{\bar\lambda},t\right)}\end{pmatrix},\quad \hat{\vec{\psi}}_n(\lambda,t)=(-1)^n\begin{pmatrix}\psi_{1n}(-\lambda,t)\\ -\psi_{2n}(-\lambda,t)\end{pmatrix} \tag{7}$$

are also a solution of (4).

The inverse scattering transform (IST) [5, 78] of the AL equation (1) for localized initial data was developed in [2, 3] (see [6] for the IST of vector generalizations of the AL equations). For the IST of the AL equations for non zero boundary conditions see [1, 14, 60, 64, 65, 74]. The finite gap method (FG) [24, 39, 40, 46, 57] for periodic and quasi-periodic AL solutions was developed in [53].

It is well-known that the homogeneous background solutions of the NLS equation (3)

$$a\exp\left(2i\eta|a|^2\tau\right),\quad a \text{ complex constant parameter}, \tag{8}$$

is unstable under the perturbation of waves with sufficiently large wave length in the focusing case $\eta=1$ [9, 10, 77, 80], and always stable in the defocusing case $\eta=-1$, and the modulation instability (MI) of the focusing case is the main cause for the formation of anomalous (rogue) waves (AWs) [25, 34, 42, 43, 59, 61, 80]. Since (8) is also the exact homogeneous solution of the AL equation (replacing τ by t), it is natural to investigate their linear instability properties under monochromatic perturbations with respect to the AL dynamics, and study how such instability develops into the full nonlinear regime.

We remark that, as in the NLS case, the AL equations have the elementary gauge symmetry (if u is solution, also $\tilde u_n=u_n\exp(i\rho),\ \rho\in\mathbb{R}$ is solution); then a could be chosen to be positive without loss of generality (but we shall not do it here). Unlike the NLS case, for which, if $v(\xi,\tau)$ is a solution, also $\tilde v(\xi,\tau)=b\,v(b\xi,b^2\tau),\ b\in\mathbb{R}$ is solution), the AL equations do not possess any obvious scaling symmetry. It follows that a in (8) cannot be rescaled away as in the NLS case. Therefore one expects that, unlike the NLS case, the amplitude a of the background (8) play a crucial role in its stability properties under perturbation.

In the NLS Cauchy problem for a localized perturbation of the exact background (8), slowly modulated periodic oscillations described by the elliptic solution of (3), for $\eta=1$, play a relevant role in the longtime regime [11, 12]. These features are universal and can be observed also in the focusing AL equation [13].

The Cauchy problem of the periodic AWs of the focusing NLS equation (3) has been solved in [28, 31], to leading order and in terms of elementary functions, for generic periodic initial perturbations of the unstable background:

$$\begin{aligned} &v(\xi,0)=a\left(1+\varepsilon w(\xi)\right),\ 0<\varepsilon\ll 1,\ w(\xi+L)=w(\xi),\\ &w(\xi)=\textstyle\sum_{j=1}^{\infty}\left(c_j e^{ik_j\xi}+c_{-j}e^{-ik_j\xi}\right),\ \ k_j=\frac{2\pi}{L}j, \end{aligned} \tag{9}$$

in the case of a finite number N of unstable modes, using a suitable adaptation of the FG method. In the simplest case of a single unstable mode ($N=1$), the above FG solution provides the analytic and quantitative description of an ideal Fermi–Pasta–Ulam–Tsingou (FPUT) recurrence [26] without thermalization, of periodic NLS AWs over the unstable background (8), described, to leading order, by the well-known Akhmediev breather (AB)

$$\begin{aligned} &\mathcal{A}\left(\xi,\tau;k,\tilde X,\tilde T,\rho\right)=\tilde a e^{2i|\tilde a|^2\tau+i\rho}\,\frac{\cosh\left[\tilde\sigma(k)\left(\tau-\tilde T\right)+2i\phi\right]+\sin\phi\,\cos\left[k\left(\xi-\tilde X\right)\right]}{\cosh\left[\tilde\sigma(k)\left(\tau-\tilde T\right)\right]-\sin\phi\,\cos\left[k\left(\xi-\tilde X\right)\right]},\\ &\tilde\sigma(k):=k\sqrt{4|\tilde a|^2-k^2}, \end{aligned} \tag{10}$$

solution of focusing NLS for the arbitrary real parameters $\tilde a,\rho,k,\tilde X,\tilde T$, but with different parameters at each appearance [28]. See also [30] for an alternative and effective approach to the

study of the AW recurrence in the case of a single unstable mode, based on matched asymptotic expansions; see [33] for a FG model describing the numerical instabilities of the AB and [32] for the analytic study of the linear, nonlinear, and orbital instabilities of the AB within the NLS dynamics; see [29] for the analytic study of the phase resonances in the AW recurrence; see [66] and [19] for the analytic study of the FPUT AW recurrence in other NLS type models: respectively the PT-symmetric NLS equation [4] and the massive Thirring model [52, 72], showing the universality of the above behavior. The AB, describing the nonlinear instability of a single mode, and its N-mode generalization were first derived respectively in [8] and [41]. The NLS recurrence of AWs in the periodic setting has been investigated in several numerical and real experiments, see, f.i., [44, 54, 63, 75, 76], and qualitatively studied in the past via a three-wave approximation of NLS [36, 73].

In addition, a perturbation theory describing analytically how the FPUT recurrence of AWs is modified by the presence of a perturbation of NLS has been recently introduced in [15], in the simplest case of a small linear loss or gain, giving a theoretical explanation of previous interesting real and numerical experiments [44, 69]. This theory has been applied in [18] to the complex Ginzburg-Landau [56] and Lugiato–Lefever [49] models, treated as perturbations of NLS (see also [16]).

These results suggest two interesting problems.

(i) the construction of the analytic and quantitative description of the dynamics of periodic AWs of the AL lattices;
(ii) the understanding of the effect of a perturbation of the AL lattices on such a dynamics.

The solution of the first problem is the main goal of this paper; the solution of second problem is contained in [20].

We remark that the established terminology 'focusing' and 'defocusing' AL equation (1) for respectively the cases $\eta = 1$ and $\eta = -1$ is certainly adeguate whenever the NLS continuous limits (2) is possible. But the AL lattice for $\eta = -1$ and sufficiently large amplitudes cannot reduce to the defocusing NLS equation (3) in the continuous limit, and its focusing/defocusing properties have to be clarified. As we shall see in the following, (i) not only the homogeneous background is modulationally unstable, but this MI leads to blow up at finite time; (ii) the proper continuous limit describing this case is a novel focusing NLS equation with nonlinear and weak dispersion, making evident that this regime is strongly focusing. Therefore we feel, from physical considerations, that the term 'defocusing' would not be appropriate in this case, and we prefer to use the neutral terminology $AL_{\pm}$.

The paper is organized as follows. In section 2 we investigate the linear stability properties of the background (8), extending results already present in the literature [7, 58], and showing that, unlike the NLS case, the background of AL_{-} is unstable under any monochromatic perturbation if $|a| > 1$. In section 3 we present the exact solutions of $AL_{\pm}$ describing the instability of one and two unstable modes, and we show that: (i) the solutions of AL_{+} are always regular, but with an amplitude, relative to the background, growing as $|a|^2$ and as $|a|^4$ respectively in the case of one and two unstable modes; (ii) the solutions of AL_{-} develop singularities in closed curves of spacetime, and when these curves intersect a line $x = n_0 \in \mathbb{Z}$ (the generic case), the solution blows up at finite time in the site $n = n_0$. Motivated by these last features, we construct the continuous limits of the AL equations exhibiting the same features, and showing clearly that the case $\eta = -1$ is focusing for sufficiently large amplitudes. In section 4 we use the matched asymptotic expansion approach developed in [30] to solve to leading order the periodic Cauchy problem of the AWs, (i) describing in terms of elementary functions the associated AW recurrence of one and two unstable modes (in this second case for non generic

initial perturbations) in the AL_+ model; (ii) showing analytically how a smooth perturbation blows up at finite time in the AL_- model. Section 5 is dedicated to conclusions and future perspectives. In the appendix we construct the exact solutions studied in section 3 using the Darboux transformations (DTs) of $AL_\pm$ [27].

To the best of our knowledge, known results concerning AWs of the AL models prior to our work are the following. The exact solution over the background, corresponding to a spectral parameter in general position, and containing as limiting cases the discrete analogues of the Akhmediev breather (24), of the Kuznetsov–Ma [47, 50] and Peregrine [62] solutions, was first constructed in [55] for $\eta = 1$ and in [60] for $\eta = -1$. The amplitude growth of (24) for large $|a|$ was investigated in [7], together with the linear instability properties of the background solution of AL_+. Numerical experiments for the Cauchy problem of AWs for AL_+ are reported in [68]. The linear instability properties of the background solution for $\eta = -1$ were investigated for Peregrine type solutions of any order in [58], using the Hirota method [35].

2. Linear stability properties of the background in the AL case

To study the (linear) stability properties of the background solutions (8) in the $AL_\pm$ dynamics, we seek solutions of (1) in the form

$$u_n(t) = a e^{2i\eta|a|^2 t}\left(1 + \epsilon\xi_n(t) + O\left(\epsilon^2\right)\right), \quad 0 < \epsilon \ll 1, \tag{11}$$

obtaining, at $O(\epsilon)$, the linearized $AL_\pm$ equations for ξ_n:

$$i\dot{\xi}_n + \left(1 + \eta|a|^2\right)\left(\xi_{n+1} + \xi_{n-1}\right) - 2\xi_n + 2\eta|a|^2\overline{\xi_n} = 0, \quad \eta = \pm 1. \tag{12}$$

If the perturbation is a monochromatic wave:

$$\xi_n(t) = \gamma_+(t)\, e^{i\kappa n} + \gamma_-(t)\, e^{-i\kappa n}, \tag{13}$$

Equation (12) reduces to the system of ODEs

$$\begin{aligned} &i\dot{D} + 2\left[\left(1 + \eta|a|^2\right)\cos\kappa - \left(1 - \eta|a|^2\right)\right] S = 0, \\ &i\dot{S} + 2\left(1 + \eta|a|^2\right)(\cos\kappa - 1)\, D = 0, \\ &S := \gamma_+ + \overline{\gamma_-}, \quad D := \gamma_+ - \overline{\gamma_-}. \end{aligned} \tag{14}$$

whose solution reads:

$$S(t) = \nu e^{\sigma t} + \mu e^{-\sigma t}, \quad D(t) = \frac{i\sigma\left(\nu e^{\sigma t} - \mu e^{-\sigma t}\right)}{2\left(1 + \eta|a|^2\right)(1 - \cos\kappa)}, \tag{15}$$

where

$$\sigma(\kappa) = 2\sqrt{\left(1 + \eta|a|^2\right)(1 - \cos\kappa)\left[\left(1 + \eta|a|^2\right)\cos\kappa - \left(1 - \eta|a|^2\right)\right]}, \tag{16}$$

and ν, μ are two arbitrary complex parameters. From now on we fix the following constraint on the wave number

$$0 < \kappa < \pi, \tag{17}$$

since the negative values are covered by the second exponential in (11), and the growth rate (16) depends on κ through $\cos\kappa$.

The growth rate (16) implies the following stability features of the background solutions (8) of the $AL_\pm$.

The case $\eta = -1$. Equation AL_- reduces to the defocusing NLS in the continuous limit, for which the background (8) is stable under a perturbation of any wave number. The stability properties of the AL_- background are much richer [58]; indeed we distinguish three sub-cases:

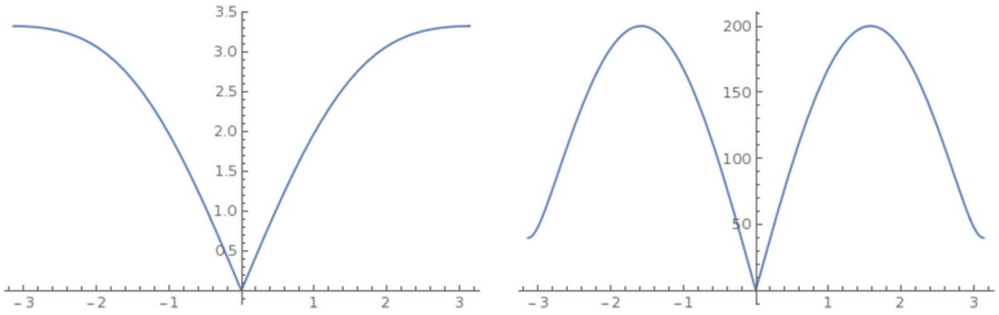

Figure 1. For $\eta=-1$ and $|a|>1$ the perturbation is unstable with exponential growth. The graph of the growth rate $\sigma(\kappa)$ in the basic period $\kappa\in(-\pi,\pi)$. In the left picture: $a=1.3<\sqrt{2}$; in the right one: $|a|=10>\sqrt{2}$.

- $|a|>1\Rightarrow\sigma>0\Rightarrow$ exponential growth and linear instability $\forall\ \kappa$ (see figure 1);
- $|a|=1\Rightarrow\sigma=0,\ S(t)=S_0,\ D(t)=-4iS_0t+D_0\Rightarrow$ instability if $S_0\neq 0$ with linear growth, stability otherwise, $\forall\ \kappa$;
- $0<|a|<1\Rightarrow\sigma\in i\mathbb{R}\Rightarrow$ oscillations and neutral stability $\forall\ \kappa$.

Since σ depends on κ through $\cos\kappa$, these stability properties are 2π-periodically extended to the whole real κ axis, with basic period $(-\pi,\pi)$. In the unstable case $|a|>1$, there are two subcases:

(i) $1<|a|<\sqrt{2}$, then $\sigma(k)$ has its absolute minimum at $\kappa=0$ with $\sigma(0)=0$, and absolute maxima at $\kappa=\pm\pi$, with $\sigma(\pm\pi)=4\sqrt{|a|^2-1}$.

(ii) $|a|>\sqrt{2}$, then $\sigma(k)$ has its absolute minimum at $\kappa=0$ with $\sigma(0)=0$, relative minima at $\kappa=\pm\pi$, with $\sigma(\pm\pi)=4\sqrt{|a|^2-1}$, and absolute maxima at $\kappa_\pm=\pm\arccos(\frac{1}{1-|a|^2})$, with $\sigma(\kappa_\pm)=2|a|^2$ (see figure 1).

The case $\eta=1$. The AL_+ equation reduces to the focusing NLS (3) in the continuous limit, for which the background (8) is unstable for monochromatic perturbations of wave number k such that $|k|<2|a|$, and the parameter a can be rescaled away due to the scaling and trivial gauge symmetries of NLS. Also in this case the stability properties of the AL background are richer than those of the NLS background, since now the amplitude $|a|$ cannot be rescaled away, and is involved in the following nontrivial way.

Define κ_a as [7]

$$\kappa_a:=\arccos\left(\frac{1-|a|^2}{1+|a|^2}\right)>0,\quad 0<\kappa_a<\pi\,; \tag{18}$$

(see figure 2); then

- if $|\kappa|<\kappa_a$ $(\cos\kappa>\frac{1-|a|^2}{1+|a|^2})$, $\sigma>0\Rightarrow$ instability with exponential growth. The growth rate has maxima at $\pm\kappa_M$, with $\kappa_M=\arccos(\frac{1}{|a|^2+1})$ and $\sigma(\pm\kappa_M)=2|a|^2$. The instability curve is similar to that of focusing NLS, except for the 2π periodicity (see figure 2).
- if $|\kappa|=\kappa_a$ $(\cos\kappa=\frac{1-|a|^2}{1+|a|^2})\Rightarrow\sigma=0, D=D_0,\ S=-4i|a|^2D_0t+S_0\Rightarrow$ instability with linear growth if $D_0\neq 0$, otherwise stability;
- if $|\kappa|>\kappa_a$ $\left(\cos\kappa<\frac{1-|a|^2}{1+|a|^2}\right)\Rightarrow\sigma\in i\mathbb{R}\Rightarrow$ linear stability and small oscillations.

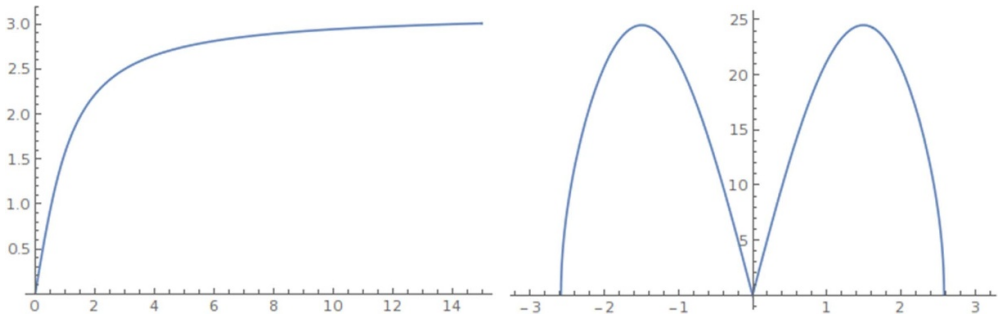

Figure 2. Left: the critical wave number κ_a as function of the amplitude $|a|$, with $\kappa_0 = 0$ and $\kappa_\infty = \pi$. Right: the growth rate, 2π-periodic in κ, has support for $|\kappa| < \kappa_a$ inside the basic periodicity interval $(-\pi, \pi)$. Here $|a| = 3.5$.

As before, these stability properties are 2π-periodically extended to the whole real κ axis.

Summarizing the results of this section, we have the following 'instability regions' of the background (8):

$$\begin{aligned} &|\kappa| < \kappa_a := \arccos\left(\tfrac{1-|a|^2}{1+|a|^2}\right),\ \forall |a| > 0, && \text{if } \eta = 1, \\ &|a| > 1,\ \forall \kappa, && \text{if } \eta = -1, \end{aligned} \tag{19}$$

where κ_a is the smallest positive branch of arccos. They were found in [7] for $\eta = 1$, and in [58] for $\eta = -1$.

As we shall see in the following, in all the cases discussed above in which the background (8) is unstable, we find it convenient to introduce the parameter ϕ defined by

$$\cos\phi = \sqrt{1 + \frac{\eta}{|a|^2}}\,\sin\left(\frac{\kappa}{2}\right), \quad 0 < \phi < \pi/2. \tag{20}$$

We remark that ϕ is real in both unstable cases (19) (it is therefore an angle) and, in terms of it, the growth rate σ (16) takes the same simple form

$$\sigma = 2|a|^2 \sin(2\phi) > 0, \tag{21}$$

as in the NLS case [28, 30, 31].

It is easy to verify, from (14), (15), and (20), that the perturbation ξ_n in (13) reads

$$\xi_n(t) = \frac{1}{\sin(2\eta\phi)}\left[|\alpha| e^{\sigma t + i\eta\phi}\cos\left[\kappa\left(x - X^+\right)\right] + |\beta| e^{-\sigma t - i\eta\phi}\cos\left[\kappa\left(x - X^-\right)\right]\right], \tag{22}$$

where

$$X^+ = \tfrac{\arg\alpha + \pi/2}{\kappa},\ \ X^- = \tfrac{-\arg\beta + \pi/2}{\kappa}, \tag{23}$$

and the arbitrary complex parameters α, β are expressed in terms of ν, μ as follows: $\alpha = -2i\sin(\eta\phi)\,\overline{\nu}$, $\beta = 2i\sin(\eta\phi)\,\mu$.

3. Exact periodic AW solutions of the AL equations

Since the background solution (8) is linearly unstable under monochromatic perturbations in the cases (19), it is important to describe how the corresponding exponential growth evolves into the nonlinear stage of MI described by the full nonlinear model. In this section we present the exact periodic solutions of $AL_\pm$ describing the nonlinear instability of a single nonlinear

mode and of two interacting nonlinear modes. The construction of these solutions using the DTs of the AL equations [27] is presented in the appendix.

3.1. The case of a single unstable mode

The instability of a single nonlinear mode K_1 of $AL_\pm$ is described by the solution:

$$\mathcal{N}_1(n,t;K_1,X_1,T_1,\rho,\eta) = ae^{2i\eta|a|^2t+i\rho}\,\frac{\cosh\left[\sigma(K_1)(t-T_1)+2i\eta\theta_1\right]+\eta G_1\cos\left[K_1(n-X_1)\right]}{\cosh\left[\sigma(K_1)(t-T_1)\right]-\eta G_1\cos\left[K_1(n-X_1)\right]}, \tag{24}$$

where

$$G_1 = \frac{\sin\theta_1}{\cos\left(\frac{K_1}{2}\right)}, \tag{25}$$

K_1 is the wave number and $\sigma(K_1)$, defined in (16), is the growth rate of the linearized theory in the unstable cases (19), the angle θ_1 is defined as in (20)

$$\cos\theta_1 = \sqrt{1+\frac{\eta}{|a|^2}}\,\sin\left(\frac{K_1}{2}\right), \tag{26}$$

and X_1, T_1 and ρ are arbitrary real parameters. Since θ_1 is defined in terms of (K_1,a,η), the growth rate $\sigma(K_1)$ and the parameter G_1 can be expressed in terms of (K_1,a,η) or in terms of (θ_1,a,η) in the following way:

$$\begin{aligned}
&\sigma(K_1) = 2\sqrt{(1+\eta|a|^2)(1-\cos K_1)\left[(1+\eta|a|^2)\cos K_1-(1-\eta|a|^2)\right]} = 2|a|^2\sin(2\theta_1),\\
&G_1 = \frac{\sin\theta_1}{\cos\left(\frac{K_1}{2}\right)} = \sqrt{1-\frac{\eta}{|a|^2}\,\frac{1-\cos K_1}{1+\cos K_1}} = \frac{\sqrt{|a|^2+\eta}\sin\theta_1}{\sqrt{|a|^2\sin^2\theta_1+\eta}}.
\end{aligned} \tag{27}$$

If $\eta=1$, (24) is the Narita solution [55] of AL_+, discrete analogue of the AB solution (10) of focusing NLS, reducing to it through the scaling

$$\begin{aligned}
&a\sim h\,\tilde{a},\ K_1\sim h\,k\ \Rightarrow\ \sigma(K_1)\sim h^2\tilde{\sigma}(k),\ G_1\sim\sin\phi,\ \ h\ll 1,\\
&\xi\sim hn,\ \tau\sim h^2t,\ \tilde{X}\sim hX,\ \tilde{T}\sim h^2T,\ \ h\ll 1,
\end{aligned} \tag{28}$$

where h is the lattice spacing. If $\eta=-1$, (24) describes the MI present in the model for sufficiently large amplitudes [60].

The solution (24) oscillates in n and is exponentially localized over the background in t in the following way

$$\mathcal{N}_1(n,t;K_1,X_1,T_1,\rho,\eta)\to ae^{2i\eta|a|^2t\pm 2i\eta\phi+i\rho},\quad \text{as}\quad t\to\pm\infty. \tag{29}$$

To study its behavior, we first replace $n\in\mathbb{Z}$ by $x\in\mathbb{R}$ in (figure 3); it is legitimate, observing that function $\mathcal{N}_1(x,t;K_1,X_1,T_1,\rho,\eta)$ solves $AL_\pm$ with n replaced by x:

$$\begin{aligned}
&iu_t+u^++u^--2u+\eta|u|^2(u^++u^-)=0,\ \ \eta=\pm1,\\
&u=u(x,t)\in\mathbb{C},\ \ u^\pm=u(x\pm1,t),\ \ u_t=\tfrac{\partial u}{\partial t},\ \ x,t\in\mathbb{R}.
\end{aligned} \tag{30}$$

If $\eta=1$, equation (26) implies that $\sin\theta_1<\cos(K_1/2)$ and equation (25) that $G_1<1$. It follows that the denominator of $\mathcal{N}_1$ is always positive. Therefore the solution $\mathcal{N}_1$ is always regular in the (x,t) plane for all values of its arbitrary parameters, like in the NLS case. But there is an important difference, since now the maximum of the absolute value of the solution (24), reached at the point $(x,t)=(X_1,T_1)$, reads [7]:

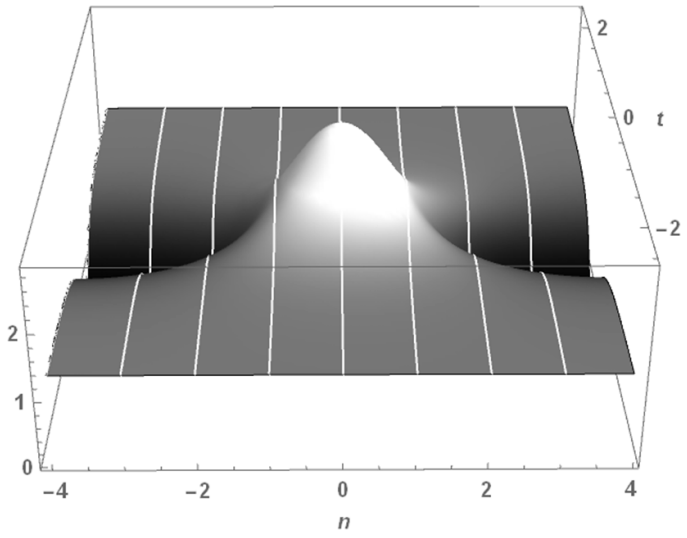

Figure 3. 3D plot of $|\mathcal{N}_1|$ for $\eta = 1$, $a = 1.3$, $K_1 = 2\pi/8$, $X_1 = T_1 = 0$.

$$\begin{aligned} Max &:= \max_{(x,t)\in\mathbb{R}^2} |\mathcal{N}_1(x,t;K_1,X_1,T_1,\rho,1))| = |\mathcal{N}_1(X_1,T_1;K_1,X_1,T_1,\rho,1)| \\ &= |a| \left| \frac{\cos(2\theta_1)+G_1}{1-G_1} \right| = |a| \left[2\left(1+|a|^2\right)\cos\left(\frac{K_1}{2}\right)\left(\sin\theta_1+\cos\left(\frac{K_1}{2}\right)\right)-1 \right], \end{aligned} \tag{31}$$

implying that the relative maximum (the ratio of the maximum of the amplitude of (24) to the background amplitude $|a|$) grows as $O(|a|^2)$ for $|a| \gg 1$:

$$\frac{Max}{|a|} = 4|a|^2\cos^2\left(\frac{\kappa}{2}\right)\left[1+O\left(|a|^{-2}\right)\right], \quad a \gg 1, \tag{32}$$

unlike the NLS case, for which $Max/|a| = 1+2\sin\phi$ does not depend on a. We remark that, if $X_1 \notin \mathbb{Z}$, the maximum of $|\mathcal{N}_1|$ is not reached in a lattice point (see figure 3).

If $\eta = -1$, equation (26) implies that $\sin\theta > \cos(K_1/2)$ and equation (25) that $G_1 > 1$. Therefore the solution (24) is singular on the closed curve $\mathcal{C}$ of the (x,t) plane defined by the equation

$$\cosh\left[\sigma\left(t-T_1\right)\right] = G_1\cos\left[\kappa\left(x-X_1\right)\right]; \tag{33}$$

this curve is centered at (X_1,T_1) and x-periodic with period $2\pi/K_1$ (see figure 4). If

$$|x-X_1| < \frac{\arccos\left(1/G_1\right)}{K_1}, \tag{34}$$

the solution $\mathcal{N}_1$ blows up at the two points $(x,t^{\pm}(x))$:

$$t^{\pm}(x) = T_1 \pm \frac{\cosh^{-1}\left(G\cos\left[\kappa\left(x-X_1\right)\right]\right)}{\sigma}; \tag{35}$$

where arccos is here the smallest positive branch of the inverse of cos, and $\cosh^{-1}$ is the positive branch of the inverse of cosh (see figure 4).

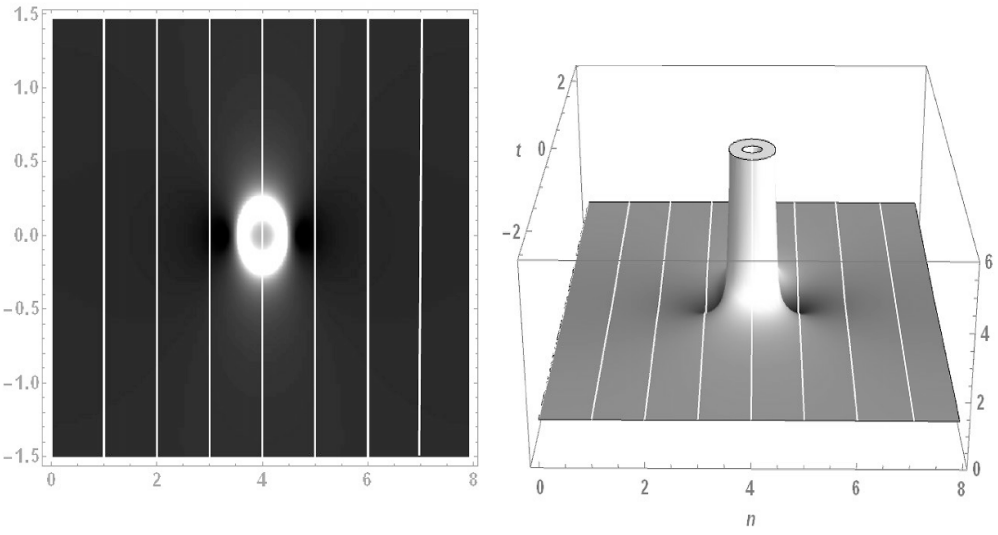

Figure 4. Density and 3D plots of the singular solution $|\mathcal{N}_1|$ of AL_-, where $a = 1.3$, $K_1 = 2\pi/8$, $T_1 = 0$, $X_1 = 4$.

We remark that the extension l of the singular curve (33) in the x direction is less than 1, since:

$$l = \frac{2}{K_1}\arccos\left(\frac{1}{G_1}\right) < 1 \quad \Leftrightarrow \quad \frac{1}{\sin\theta_1} > 1. \tag{36}$$

Consequently, if n_X is the integer closest to X_1 and

$$|n_X - X_1| > \frac{\arccos(1/G_1)}{K_1}, \tag{37}$$

then the appearance of the AW is not singular on the lattice, since the singular curve is located in the region between two subsequent sites. But this situation is not generic, and the solutions can be arbitrarily large if the singular curve is close enough to a site of the lattice.

3.2. *The case of two unstable modes*

The instability of two nonlinearly interacting modes K_1 and K_2 is described by the novel (to the best of our knowledge) two-mode solution of $AL_\pm$:

$$\mathcal{N}_2(n,t;K_1,K_2,X_1,X_2,T_1,T_2,\rho,\eta) = a\,e^{2i\eta|a|^2t+i\rho}\,\frac{N(n,t)}{D(n,t)}, \tag{38}$$

where

$$\begin{aligned} N(n,t) = {} & \cosh\left[\Sigma_1(t-T_1)+\Sigma_2(t-T_2)+2i\eta(\theta_1+\theta_2)\right] \\ & + \left(a_{12}(K_1,K_2)\right)^2\cosh\left[\Sigma_1(t-T_1)-\Sigma_2(t-T_2)+2i\eta(\theta_1-\theta_2)\right] \\ & + 2a_{12}(K_1,K_2)\left\{G_2\cosh\left[\Sigma_1(t-T_1)+2i\eta\theta_1\right]\cos\left[K_2(n-X_2)\right]\right. \\ & \left. + G_1\cosh\left[\Sigma_2(t-T_2)+2i\eta\theta_2\right]\cos\left[K_1(n-X_1)\right]\right\} \end{aligned}$$

$$+ b_{12}^{-}(K_1,K_2)\cos\left[K_1(n-X_1)+K_2(n-X_2)\right]$$
$$+ b_{12}^{+}(K_1,K_2)\cos\left[K_1(n-X_1)-K_2(n-X_2)\right], \tag{39}$$

$$\begin{aligned} D(n,t) = {} & \cosh\left[\Sigma_1(t-T_1)+\Sigma_2(t-T_2)\right] + \left(a_{12}(K_1,K_2)\right)^2 \cosh\left[\Sigma_1(t-T_1)-\Sigma_2(t-T_2)\right] \\ & - 2a_{12}(K_1,K_2)\left\{G_2\cosh\left[\Sigma_1(t-T_1)\right]\cos\left[K_2(n-X_2)\right]\right. \\ & \left. + G_1\cosh\left[\Sigma_2(t-T_2)\right]\cos\left[K_1(n-X_1)\right]\right\} \\ & + b_{12}^{-}(K_1,K_2)\cos\left[K_1(n-X_1)+K_2(n-X_2)\right] \\ & + b_{12}^{+}(K_1,K_2)\cos\left[K_1(n-X_1)-K_2(n-X_2)\right], \end{aligned} \tag{40}$$

and where

$$\begin{aligned} & \cos\theta_j = \sqrt{1+\tfrac{\eta}{|a|^2}}\sin\left(\tfrac{K_j}{2}\right), \quad j=1,2, \\ & G_j = \tfrac{\sin(\theta_j)}{\cos\left(\frac{K_j}{2}\right)}, \quad j=1,2, \\ & \Sigma_j = \sigma(K_j) = 2|a|^2\sin(2\theta_j), \quad j=1,2, \\ & a_{12} = \tfrac{\sin(\theta_1+\theta_2)}{\sin(\theta_1-\theta_2)}, \end{aligned} \tag{41}$$

$$b_{12}^{\pm} = \tfrac{\sin(\theta_1)\sin(\theta_2)}{\sin^2(\theta_1-\theta_2)}\left(\sqrt{\tfrac{\cos\left(\frac{K_2}{2}\right)}{\cos\left(\frac{K_1}{2}\right)}}\cos(\theta_1) \pm \sqrt{\tfrac{\cos\left(\frac{K_1}{2}\right)}{\cos\left(\frac{K_2}{2}\right)}}\cos(\theta_2)\right). \tag{42}$$

Also this solution oscillates in n and is exponentially localized in time over the background:

$$\mathcal{N}_2(n,t;K_1,K_2,X_1,X_2,T_1,T_2,\rho,\eta) \to a\,e^{2i\eta|a|^2t+i[\rho\pm2\eta(\theta_1+\theta_2)]}, \quad as\ \ t\to\pm\infty.$$

In the rest of the paper we shall limit our considerations to the case $K_2 = 2K_1$; then the solution is periodic with period $2\pi/K_1$.

As in the case of a single mode, in the natural continuous limit (see (28)) the solution for $\eta = 1$ reduces to the two breather solution of Akhmediev type [30], while it does not have a continuous limit in the case $\eta = -1$.

As in the case of a single mode, it is possible to show the following.
(i) If $\eta = 1$, the solution (38) is always regular. If $|T_1 - T_2| > O(1)$ the two nonlinear modes are separated into two weakly interacting Narita solutions with wave numbers K_1 and K_2. If $|T_1 - T_2| \ll 1$ the two nonlinear modes appear almost at the same time interacting nonlinearly. If $T_1 = T_2$, $K_2 = 2K_1$, and $X_2 = X_1 + \frac{2\pi}{4K_1}$ the two modes are amplitude-locked and phase-locked in a characteristic configuration similar to the one of NLS (see figure 5).

The maximum height of $|\mathcal{N}_2|$ can be calculated in terms of elementary functions in two cases: when $|T_1 - T_2| \gg 1$ and the solution describes two separated Narita solutions (24), and when they are amplitude- and phase-locked:

$$T_1 = T_2, \quad X_2 = X_1 + \frac{2\pi}{4K_1}. \tag{43}$$

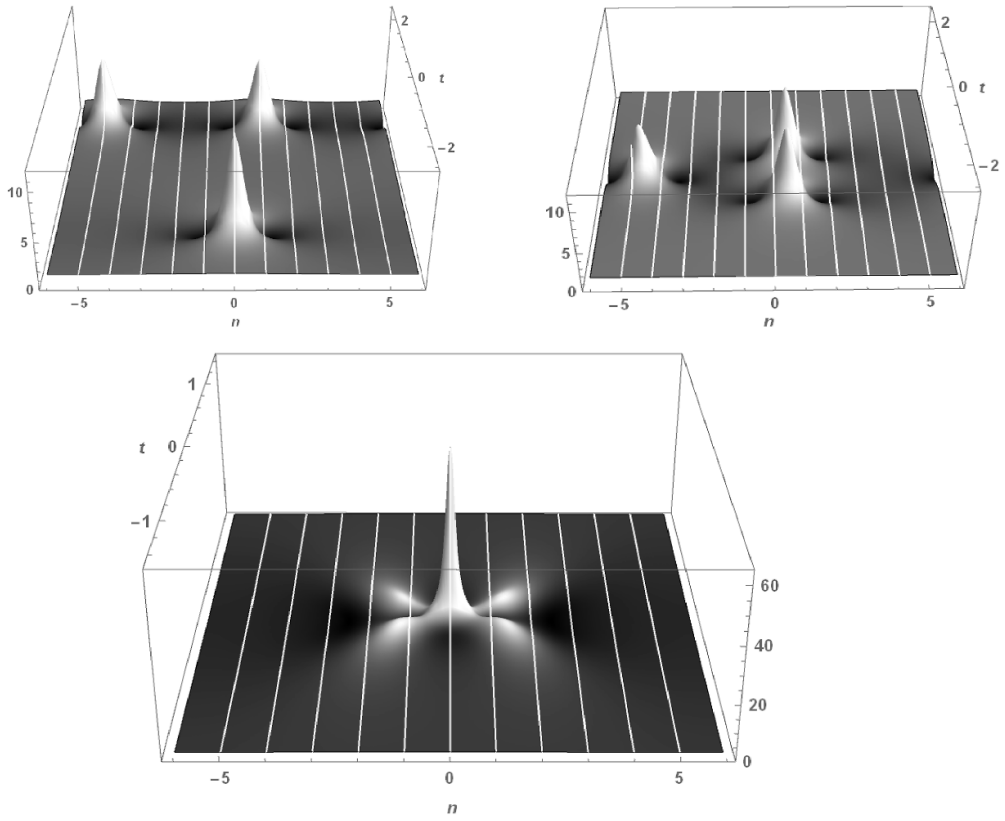

Figure 5. 3D plots of $|\mathcal{N}_2|$ for $\eta = 1$, $a = 1.3$, $K_1 = 2\pi/12$, and $K_2 = 2K_1$. Top left: $T_1 = -1$, $T_2 = 1.5$, $X_1 = 0$ and $X_2 = 1$. $|T_2 - T_1| \geqslant 1$, and the solution appears as two separate Narita solutions of wave numbers K_1 and K_2. Top right: $T_1 = T_2 = 0$, $X_1 = 0$ and $X_2 = 1$. Since $T_1 = T_2$, the two modes appear together and strongly interact. Bottom: the phase locking choice of the parameters: $T_1 = T_2 = 0$, $X_1 = 0$ and $X_2 = X_1 + \frac{2\pi}{4K_1} = 3$.

In the second case, the maximum height reached by the solution is given by:

$$\begin{aligned}\max\left|\mathcal{N}_2\right| &= |\mathcal{N}_2\left(X_1,T_1;K_1,K_2,X_1,X_1\pm\frac{2\pi}{4K_1},T_1,T_1,\rho,1\right)\Big| \\ &= |a|\left[2\left(1+|a|^2\right)\cos\left(\frac{K_1}{2}\right)\left(\cos\left(\theta_1\right)+\cos\left(\frac{K_1}{2}\right)\right)-1\right] \\ &\quad\times\left[2\left(1+|a|^2\right)\cos\left(\frac{K_2}{2}\right)\left(\cos\left(\theta_2\right)+\cos\left(\frac{K_2}{2}\right)\right)-1\right], \qquad (44)\end{aligned}$$

implying that the maximum amplitude of $|\mathcal{N}_2|$, relative to the background, grows as $|a|^4$ for $|a|$ large: $\max|\mathcal{N}_2|/|a| = O\left(|a|^4\right)$, $|a| \gg 1$ (see the last of figure 5).

(ii) If $\eta = -1$, $\mathcal{N}_2$ develops always singularities at finite time on three closed curves of the (x,t) plane; one curve for the mode K_1 and two curves for K_2 (see figure 6).

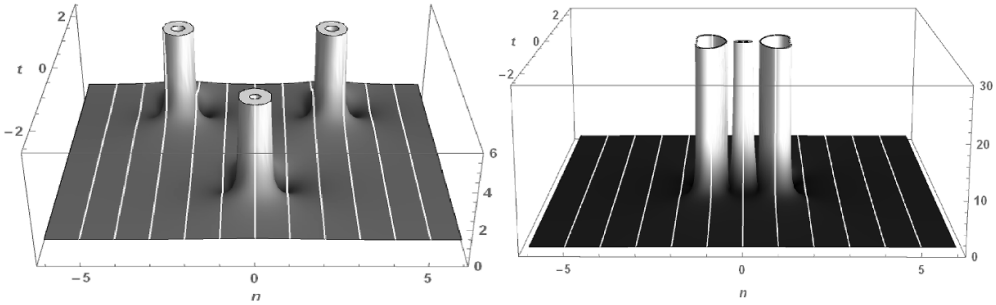

Figure 6. 3D plots of $|\mathcal{N}_2|$ for $\eta=-1$, $a=1.3$, $K_1=2\pi/12$, $K_2=2K_1$. Left: $T_1=0$, $T_2=1$, $X_1=0$ and $X_2=3$. Since $|T_1-T_2|=1$, the solution describes two separate weakly interacting singular solutions of the type $\mathcal{N}_1$, with modes K_1 and $K_2=2K_1$. Right: $T_1=T_2=0$, $X_1=0$ and $X_2=X_1+\frac{2\pi}{4K_1}=3$ (the phase-locking choice of the parameters).

3.3. *Another continuous limit of the AL equations*

We remark that the AW solutions (24) and (38) for $\eta=-1$ do not have a continuous limit to defocusing NLS, since the instability condition $|a|>1$ is not consistent with the limit (2). This fact strongly suggests to explore the following different continuous limits of the AL equations

$$\begin{aligned} &u_n(t)=w(\xi,\tau), \quad hn=\xi, \quad \tau=t, \quad 0<h\ll 1,\\ &u_n(t)=w(\xi,\tau_1), \quad hn=\xi, \quad \tau_1=ht, \quad 0<h\ll 1, \end{aligned} \tag{45}$$

leading respectively to the following equations

$$\begin{aligned} &iw_\tau+h^2w_{\xi\xi}\left(1+\eta|w|^2\right)+2\eta|w|^2w=0, \quad \eta=\pm 1, \quad 0<h\ll 1,\\ &ihw_{\tau_1}+h^2w_{\xi\xi}\left(1+\eta|w|^2\right)+2\eta|w|^2w=0, \quad \eta=\pm 1, \quad 0<h\ll 1, \end{aligned} \tag{46}$$

up to smaller terms of order $O(h^3)$. Both equations are NLS type equations with an interesting nonlinear and weak dispersion. If $\eta=1$ the nonlinear dispersion and the self-interacting potential have the same sign; therefore we are in the focusing regime. If $\eta=-1$, as in the AL case, the situation is richer and we distinguish to cases. (i) If $|w|<1$ the nonlinear dispersion and the self-interacting potential have opposite sign and we are in the defocusing regime [17]. (ii) If $|w|>1$ the nonlinear dispersion and the self-interacting potential have the same negative sign and we are in the focusing regime; the homogeneous background is unstable, and a small periodic perturbation of it gives rise to a blow up at finite time, exactly like the AL case [17]. We expect that the continuous limit of solutions (24) and (38) should provide an analytic description of this blow up. In addition the NLS type equations (46) are quasi integrable, since they can be obtained as compatibility condition of a certain Lax pair, up to $O(h^3)$ corrections [17].

Therefore the AL equations, constructed as integrable lattice generalization of the NLS equations and reducing to them in the limit (2), possess different interesting continuous limits, like equations (46), making even more clear that the case $\eta=-1$ is defocusing only if the amplitudes are less than 1; otherwise it is focusing, and this focusing effect is so strong (now the dispersion is nonlinear) to lead to the blow up of the solution at finite time. Another interesting continuous limit is in [70].

4. AW recurrence and blow up at finite time of periodic AWs of $AL_{\pm}$

In this section we study the periodic Cauchy problem with period $N \in \mathbb{N}^+$ for $AL_{\pm}$

$$\begin{aligned} &i\dot{u}_n - 2u_n + \left(1+\eta|u_n|^2\right)(u_{n-1}+u_{n+1}) = 0, \\ &u_{n+N}(t) = u_n(t), \quad \forall n \in \mathbb{Z},\ \forall t \geqslant 0, \end{aligned} \tag{47}$$

in which the initial condition is a generic periodic perturbation of the background (8) (what we call the 'periodic AW Cauchy problem'):

$$u_n(0) = a\left(1+\epsilon\left(\sum_{j=1}^{p}\left(c_j e^{i\kappa_j n} + c_{-j}e^{-i\kappa_j n}\right) + c_0\right)\right), \quad 0<\epsilon\ll 1, \tag{48}$$

where

$$\kappa_j = \frac{2\pi}{N}j, \quad 1 \leqslant j \leqslant p, \tag{49}$$

and

$$p = \begin{cases} \frac{N}{2}, & \text{if } N \text{ is even}, \\ \frac{N-1}{2}, & \text{if } N \text{ is odd}. \end{cases} \tag{50}$$

As we shall see in the following, it is convenient to define the parameters

$$\begin{aligned} &\sigma_j = 2|a|^2\sin(2\phi_j), \\ &X_j^+ = \tfrac{\arg(\alpha_j)+\pi/2}{\kappa_j}, \quad X_j^- = \tfrac{-\arg(\beta_j)+\pi/2}{\kappa_j}, \end{aligned} \tag{51}$$

where

$$\cos\phi_j = \sqrt{1+\tfrac{\eta}{|a|^2}}\sin\left(\tfrac{\kappa_j}{2}\right), \tag{52}$$

and

$$\alpha_j := \overline{c_j}e^{-i\eta\phi_j} - c_{-j}e^{i\eta\phi_j}, \quad \beta_j = \overline{c_{-j}}e^{i\eta\phi_j} - c_j e^{-i\eta\phi_j}. \tag{53}$$

To construct the solution, to leading order and in terms of elementary functions, we use the matched asymptotic expansion technique introduced in [30] for the focusing NLS model.

4.1. The AL_+ case

We first concentrate on the case $\eta = 1$, giving rise to a recurrence of regular periodic AWs, in the case of one and two unstable modes. The instability condition $|\kappa| < \kappa_a$ implies that the first $M \leqslant p$ modes $\pm\kappa_j$, $1 \leqslant j \leqslant M$ are unstable, where

$$M := \left\lfloor \frac{N\kappa_a}{2\pi} \right\rfloor, \tag{54}$$

and $\lfloor x \rfloor$ is the largest integer less or equal to x.

From equations (11), (22) and (23) it follows that the solution of the Cauchy problem (48), for $|t| \leqslant O(1)$, reads as follows:

$$u_n(t) = a\,e^{2i|a|^2 t}\Bigg\{1+\epsilon\sum_{j=1}^{M}\left[\frac{|\alpha_j|}{\sin(2\phi_j)}e^{\sigma_j t+i\phi_j}\cos\left(\kappa_j\left(n-X_j^+\right)\right)\right.$$
$$\left.+\frac{|\beta_j|}{\sin(2\phi_j)}e^{-\sigma_j t-i\phi_j}\cos\left(\kappa_j\left(n-X_j^-\right)\right)\right]+O(\epsilon)\,\text{oscillations}\Bigg\}+O\left(\epsilon^2\right), \tag{55}$$

where σ_j, ϕ_j, $X_j^{\pm}$, α_j, β_j, $1\leqslant j\leqslant M$ are defined respectively in (51), (52), and (53). This solution grows exponentially and, when $t=O(\log(1/\epsilon))$, one enters the first nonlinear stage of MI.

4.1.1. One unstable mode. In the simplest case of one unstable mode ($M=1$) only, corresponding to the case in which the period N satisfies the inequalities

$$M=1 \quad\Leftrightarrow\quad \frac{2\pi}{\kappa_a}<N<\frac{4\pi}{\kappa_a}, \tag{56}$$

only the mode κ_1 is unstable, and the corresponding nonlinear stage of MI is described by the solution (figure 3) for a suitable choice of its arbitrary parameters, obtained using matched asymptotic expansions [30].

Matching the linearized solution (55) for $M=1$ and the exact solution (24) in the intermediate time interval $1\ll t\ll T_1=\sigma_1{}^{-1}\log(\gamma^+/\epsilon)$, $\gamma^+=O(1)>0$, we have

$$\begin{aligned} &u\sim a e^{2i|a|^2 t}\left[1+\epsilon\tfrac{|\alpha|}{\sin(2\phi_1)}e^{\sigma_1 t+i\phi_1}\cos\left[\kappa_1\left(x-X_1^+\right)\right]\right],\\ &\mathcal{N}_1\sim a e^{2i|a|^2 t}e^{i(\rho-2\theta_1)}\left[1+\epsilon\tfrac{4G_1\cos\theta_1}{\gamma_+}e^{\sigma(K_1)t+i\theta_1}\cos\left[K_1(x-X_1)\right]\right] \end{aligned} \tag{57}$$

inferring that $\rho=2\phi_1$, $K_1=\kappa_1$ (consequently $\sigma(K_1)=\sigma_1$, $\theta_1=\phi_1$), $X_1=X_1^+$, and

$$\gamma^+=\frac{2\sin^2(2\phi_1)}{|\alpha_1|\cos(\kappa_1/2)} \;\Rightarrow\; t^{(1)}=T_1=\frac{1}{\sigma_1}\log\left(\frac{\sigma_1^2}{2\epsilon|a|^4|\alpha_1|\cos(\kappa_1/2)}\right). \tag{58}$$

It follows that the Narita solution $\mathcal{N}_1(x,t,\kappa_1,X_1^+,t^{(1)},2\phi_1,1)$ describes the first appearance of the AW. To describe the recurrence of AWs, it is convenient to obtain the first appearance for negative times [30], matching the linearized solution (55) for $M=1$ and the Narita solution (24) in the time interval $1\ll|t|\ll T_0=\sigma_1{}^{-1}\log(\gamma^-/\epsilon)$, $\gamma^-=O(1)>0$, $t<0$:

$$\begin{aligned} &u\sim a e^{2i\eta|a|^2 t}\left[1+\epsilon\tfrac{|\beta_1|}{\sin(2\phi_1)}e^{-\sigma_1 t-i\phi_1}\cos\left[\kappa_1\left(x-X_1^-\right)\right]\right],\\ &\mathcal{N}_1\sim a e^{2i|a|^2 t}e^{i(\rho+2\theta_1)}\left[1+\epsilon\tfrac{4G_1\cos\theta_1}{\gamma_-}e^{-\sigma(K_1)t-i\theta_1}\cos\left[K_1(x-X_1)\right]\right], \end{aligned} \tag{59}$$

Comparison gives $\rho=-2\phi_1$, $K_1=\kappa_1$ (consequently $\sigma(K_1)=\sigma_1$, $\theta_1=\phi_1$), $X=X_1^-$, and

$$\gamma^-=\frac{2\sin^2(2\phi_1)}{|\beta_1|\cos(\kappa_1/2)} \;\Rightarrow\; t^{(0)}=-T_0=-\frac{1}{\sigma_1}\log\left(\frac{\sigma_1^2}{2|a|^4\epsilon|\beta_1|\cos(\kappa_1/2)}\right). \tag{60}$$

It follows that the solution $\mathcal{N}_1(x,t,\kappa_1,X_1^-,t^{(0)},-2\phi_1,1)$ describes the first appearance of the AW also at negative times. Comparing the two consecutive appearances at times $t^{(0)}$ and $t^{(1)}$, and using the time translation symmetry of AL_+, we infer the following periodicity law for the general recurrence of the AL_+ AWs (see [30] for more details)

$$u(x+\Delta x,t+\Delta t)=u(x,t)+O(\epsilon), \tag{61}$$

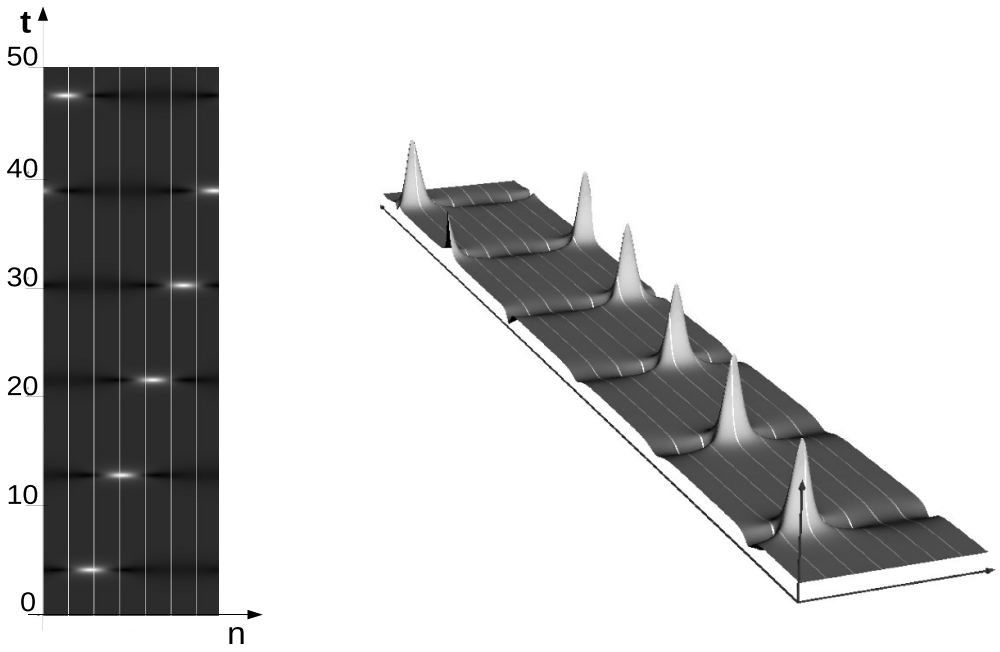

Figure 7. Density and 3D plots of $|u_n(t)|$ coming from the numerical integration of the Cauchy problem of the AWs for the AL_+ equation ($\eta = 1$), in the case of a single unstable mode. We used the 6th order Runge–Kutta method [67] with the initial condition $u_n(0) = a(1 + \epsilon(c_+ e^{ikn} + c_- e^{-ikn}))$, where $N = 7$, $a = 1.1$, $\epsilon = 10^{-4}$, $c_+ = 0.53 - i\ 0.86$ and $c_- = -0.26 + i\ 0.22$. The numerical output is in perfect quantitative agreement with the theory described by (62) and (63).

where

$$\begin{aligned} &\Delta x = X_1^+ - X_1^- = \tfrac{\arg(\alpha_1\beta_1)}{\kappa_1}, \\ &\Delta t = t^{(1)} - t^{(0)} = \tfrac{1}{\sigma_1} \log\left(\tfrac{\sigma_1^4}{4\epsilon^2|a|^8|\alpha_1\beta_1|\cos^2(\kappa_1/2)}\right). \end{aligned} \tag{62}$$

Summarizing, the nth AW appearance in the FPUT recurrence generated by the Cauchy problem (48), in the case of the single unstable mode κ_1, is described, in the time interval $|t - t^{(n)}| = O(1)$, by the Narita solution $\mathcal{N}_1(x,t;\kappa_1,x^{(n)},t^{(n)},1,\rho_n)$ up to $O(\epsilon)$ errors, where

$$\begin{aligned} &x^{(n)} = x^{(1)} + (n-1)\,\Delta x, \;\; x^{(1)} = \tfrac{\arg(\alpha_1)+\pi/2}{\kappa_1}, \quad \bmod N, \\ &t^{(n)} = t^{(1)} + (n-1)\,\Delta t, \;\; t^{(1)} = \tfrac{1}{\sigma_1}\log\left(\tfrac{\sigma_1^2}{2\epsilon|a|^4|\alpha_1|\cos(\kappa_1/2)}\right), \\ &\rho_n = 2\phi_1 + (n-1)\,4\phi_1, \end{aligned} \tag{63}$$

and Δx and Δt are defined in (62). This is the analytic and quantitative description of the FPUT recurrence of AWs of the AL_+ equation in term of the initial data through elementary functions. $x^{(1)}$ and $t^{(1)}$ are respectively the first appearance time and the position of the maximum of the absolute value of the AW; Δx is the x-shift of the position of the maximum between two consecutive appearances, and Δt is the time interval between two consecutive appearances (see figure 7).

The quantitative agreement between the above theory and numerical experiments is perfect, as one can see from the following table, in which one compares the values $(x^{(j)}, t^{(j)})$ of the position and time of the jth appearance of the AW, for $j = 1, \dots, 6$, as predicted by (62) and (63), with the values coming from the numerical experiment of figure 7. E.g., for $\epsilon = 10^{-4}$, the first disagreement in the 6th appearance is in the 7th decimal digit, corresponding to the 9th significant digit!

	Numeric	Theory
$(x^{(1)}, t^{(1)})$	(1.879 770 83, 4.178 924 77)	(1.879 770 74, 4.178 924 29)
$(x^{(2)}, t^{(2)})$	(3.084 433 57, 12.807 7003)	(3.084 433 36, 12.807 6998)
$(x^{(3)}, t^{(3)})$	(4.289 096 33, 21.436 475 86)	(4.289 095 97, 21.436 475 49)
$(x^{(4)}, t^{(4)})$	(5.493 759 10, 30.065 251 40)	(5.493 758 59, 30.065 251 08)
$(x^{(5)}, t^{(5)})$	(6.698 421 86, 38.694 026 94)	(6.698 421 21, 38.694 026 68)
$(x^{(6)}, t^{(6)})$	(0.903 084 62, 47.322 802 49)	(0.903 083 83, 47.322 802 28)

In addition, using the fact that, at each appearance, the AW is exponentially localized in time, and that, from (29), after each appearance, the background exhibits a $4\phi_1$ phase shift, the FPUT recurrence can be described by the following expression, uniform in space-time, with $t \leqslant t^{(n)} + O(1)$:

$$u(x,t) = \sum_{j=0}^{n} \mathcal{N}_1\left(x, t; \kappa_1, x^{(j)}, t^{(j)}, \rho_j, 1\right) - a e^{2i|a|^2 t} \frac{1 - e^{4i\phi_1 n}}{1 - e^{4i\phi_1}} + O(\epsilon). \tag{64}$$

We remark, from (63), that the maximum of the AW at the first appearance is located on a lattice point $x^{(1)} \in \mathbb{Z}$, if the initial data are such that

$$\frac{\arg \alpha_1}{\kappa_1} + \frac{N}{4} \in \mathbb{Z}, \tag{65}$$

If, in addition, $\Delta x \in \mathbb{Z}$, i.e. from (63) and (62)

$$\frac{\arg \beta_1}{\kappa_1} - \frac{N}{4} \in \mathbb{Z}, \tag{66}$$

then the maxima of the FPUT recurrence are all located on the lattice points.

The distinguished case $\alpha_1\beta_1 \in \mathbb{R}$. As in the NLS case, a very distinguished situation occurs when the initial data are such that

$$\alpha_1\beta_1 \in \mathbb{R}. \tag{67}$$

Indeed, from (53) and (62):

- If $\alpha_1\beta_1 > 0$, then $\Delta x = 0$ and the FPUT recurrence is periodic with period Δt.
- If $\alpha_1\beta_1 < 0$, then $\Delta x = N/2$ and the FPUT recurrence is periodic with period $2\Delta t$.

It is easy to verify that

$$\alpha_1\beta_1 \in \mathbb{R} \quad \Leftrightarrow \quad |c_1| = |c_{-1}| =: |c|, \tag{68}$$

with

$$\alpha_1\beta_1 = 2|c|^2 \left[\cos\gamma - \cos(2\phi_1)\right], \quad \gamma := \arg(c_1) + \arg(c_{-1}), \tag{69}$$

Therefore, in terms of the initial data :

- $|c_1| = |c_{-1}|,\ |\gamma| < 2\phi_1 \quad \Leftrightarrow \quad \alpha_1\beta_1 > 0,$
- $|c_1| = |c_{-1}|,\ |\gamma| > 2\phi_1 \quad \Leftrightarrow \quad \alpha_1\beta_1 < 0,$

Particularly interesting subcases are $u_n(0) \in \mathbb{R}$ and $u_n(0) \in i\mathbb{R}$.

(a) If $u_n(0) \in \mathbb{R}$, then $|c_1| = |c_{-1}|,\ \gamma = 0$, implying $\alpha_1\beta_1 > 0$, $\Delta x = 0$, and a periodic FPUT recurrence with period Δt.
(b) If $u_n(0) \in i\mathbb{R}$, then $|c_1| = |c_{-1}|,\ |\gamma| = \pi$, implying $\alpha_1\beta_1 < 0$, $\Delta x = M/2$, and a periodic FPUT recurrence with period $2\Delta t$.

We remark that the condition (67) is not generic with respect to the AL dynamics, since it arises imposing the real constraint $|c_1| = |c_{-1}|$ on the initial data. But, as we shall see in the forthcoming paper [20], it becomes the generic asymptotic state when the AL_+ dynamics is perturbed by a small loss or gain.

4.1.2. Two unstable modes. In the case of two unstable modes ($M = 2$), corresponding to the case in which the period N satisfies the inequalities

$$M = 2 \quad \Leftrightarrow \quad \frac{4\pi}{\kappa_a} < N < \frac{6\pi}{\kappa_a}, \tag{70}$$

only the modes κ_1 and κ_2 are unstable, and the corresponding nonlinear stage of MI is described by the solution $\mathcal{N}_2$ for a suitable choice of its arbitrary parameters.

Matching the linearized solution (55) for $M = 2$ and the AL_+ solution (38) in the intermediate time interval $1 \ll t \ll \left({\sigma_1}^{-1} + {\sigma_2}^{-1}\right)|\log(\epsilon))|/2$, we have

$$\begin{aligned} u &\sim a\, e^{2i|a|^2 t}\left[1 + \epsilon \sum_{j=1}^{2}\left(\tfrac{|\alpha_j|}{\sin(2\phi_j)} e^{\sigma_j t + i\phi_j}\cos\left[\kappa_j\left(n - X_j^+\right)\right]\right)\right], \\ \mathcal{N}_2 &\sim a\, e^{2i|a|^2 t} e^{i(\rho - 2(\theta_1+\theta_2))}\left[1 + \sum_{j=1}^{2}\left(\tfrac{2a_{12}\sin(2\theta_j)}{\cos\left(\frac{K_j}{2}\right)} e^{\Sigma_j(t-T_j)+i\theta_j}\cos\left[K_j\left(n - X_j\right)\right]\right)\right], \end{aligned} \tag{71}$$

inferring that $\rho = 2(\theta_1 + \theta_2)$, $K_j = \kappa_j$ (consequently $\theta_j = \phi_j$ and $\Sigma_j = \sigma_j$), $X_i = X_i^+$, for $i = 1, 2$, and

$$T_j = t_j^+ := \frac{1}{\sigma_j}\log\left(\frac{a_{12}\,\sigma_j^2}{2\epsilon|a|^4|\alpha_j|\cos\left(\kappa_j/2\right)}\right),\ j = 1, 2. \tag{72}$$

It follows that the solution $\mathcal{N}_2(n, t; \kappa_1, \kappa_2, X_1^+, X_2^+, t_1^+, t_2^+, 2(\theta_1 + \theta_2), 1)$ describes the first appearance of the AW.

Proceeding as in the case of a single unstable mode, we describe the first appearance for negative times, matching the linearized solution (22) for $M = 2$ and the solution (38) in the time interval $1 \ll |t| \ll \left({\sigma_1}^{-1} + {\sigma_2}^{-1}\right)|\log(\epsilon))|/2,\ t < 0$:

$$\begin{aligned} u &\sim a e^{2i|a|^2 t}\left[1 + \epsilon \sum_{j=1}^{2}\left(\tfrac{|\beta_j|}{\sin(2\phi_j)} e^{-\sigma_j t - i\phi_j}\cos\left[\kappa_j\left(x - X_j^-\right)\right]\right)\right], \\ \mathcal{N}_2 &\sim a\, e^{2i|a|^2 t} e^{i(\rho + 2(\theta_1+\theta_2))}\left[1 + \sum_{j=1}^{2}\left(\tfrac{2a_{12}\sin(2\theta_j)}{\cos\left(\frac{K_j}{2}\right)} e^{-\Sigma_j(t-T_j)-i\theta_j}\cos\left[K_j\left(n - X_j\right)\right]\right)\right], \end{aligned} \tag{73}$$

inferring that $\rho = -2(\theta_1+\theta_2)$, $K_j = \kappa_j$ (consequently $\theta_j = \phi_j$ and $\Sigma_j = \sigma_j$), $X_j = X_j^-$, and

$$T_j = t_j^- := -\frac{1}{\sigma_j}\log\left(\frac{a_{12}\,\sigma_j^2}{2\epsilon|a|^4|\beta_j|\cos(\kappa_j/2)}\right),\ \ j=1,2. \tag{74}$$

It follows that the solution $\mathcal{N}_2(n,t;\kappa_1,\kappa_2,X_1^-,X_2^-,t_1^-,t_2^-,1,-2(\theta_1+\theta_2),1)$ describes the first appearance of the AW at negative times. As in the one mode case, comparing the two consecutive appearances we construct the solution of the Cauchy problem to leading order. Introduce:

$$\begin{aligned}
&\Delta x_j = X_j^+ - X_j^- = \tfrac{\arg(\alpha_j\beta_j)}{\kappa_j},\quad j=1,2,\\
&\Delta t_j = t_j^+ - t_j^- = \tfrac{2}{\sigma_j}\log\left(\frac{\sigma_j^2}{2|a|^4\epsilon\sqrt{|\alpha_j\beta_j|}\cos(\kappa_j/2)}\right).
\end{aligned} \tag{75}$$

Then the nth AW appearance in the FPUT recurrence generated by the Cauchy problem, in the case of two unstable modes κ_1 and κ_2, is described, in the time interval $|t-\left(t_1^{(n)}+t_1^{(n)}\right)/2| = O(1)$, by the solution

$\mathcal{N}_2\left(n,t;\kappa_1,\kappa_2,x_1^{(n)},x_2^{(n)},t_1^{(n)},t_2^{(n)},-2(\theta_1+\theta_2),1\right)$ up to $O(\epsilon)$ errors, where

$$\begin{aligned}
&x_j^{(n)} = x_j^{(1)} + (n-1)\,\Delta x_j,\quad x_j^{(1)} = X_j^+ = \tfrac{\arg(\alpha_j)+\pi/2}{\kappa_j},\quad \mod N,\\
&t_j^{(n)} = t_j^{(1)} + (n-1)\,\Delta t_j,\quad t_j^{(1)} = t_j^+ = \tfrac{1}{\sigma_j}\log\left(\frac{\sigma_j^2}{2|a|^2\epsilon|\alpha_j|\cos(\kappa_j/2)}\right),\\
&\rho^{(n)} = 2\,(\phi_1+\phi_2) + 4\,(n-1)\,(\phi_1+\phi_2),
\end{aligned} \tag{76}$$

and Δx_j and Δt_j are defined in (62). This is the analytic and quantitative description of the FPUT recurrence of AWs of the AL equation in term of the initial data through elementary functions (see figure 8).

Equivalently, using the fact that, at each appearance, the AW is exponentially localized in time and the background exhibits a $4(\phi_1+\phi_2)$ phase shift, the FPUT recurrence can be described by the following expression, uniform in space-time, with $t \leqslant \left(t_1^{(n)}+t_1^{(n)}\right)/2 + O(1)$:

$$u(x,t) = \sum_{j=0}^{n}\mathcal{N}_2\left(n,t;\kappa_1,\kappa_2,n_1^{(j)},n_2^{(j)},t_1^{(j)},t_2^{(j)},\rho^{(j)}\right) - a\,e^{2i|a|^2t}\tfrac{1-e^{4i(\phi_1+\phi_2)n}}{1-e^{4i(\phi_1+\phi_2)}} + O(\epsilon). \tag{77}$$

It is important to remark that the recurrence results of this subsection for the case of two unstable modes are valid if the initial data are such that the first appearance times of the two unstable modes, for positive and negative t, are approximately the same: $|t_1^{(j)} - t_2^{(j)}| \ll 1$, $j = 0,1$, implying that the unstable modes appear approximately at the same time for many recurrences (see figure 8). If the appearance times of the two modes are sensibly different, the picture is more complicated and the FG approach is the proper tool to analyze it, as it was done in [31] for the NLS model.

4.2. The AL$_-$ case

If $\eta = -1$ and $|a| > 1$, all modes $\pm\kappa_j$, $1 \leqslant j \leqslant p$ are unstable, and the solution of the Cauchy problem (48), for $|t| \leqslant O(1)$, reads as follows:

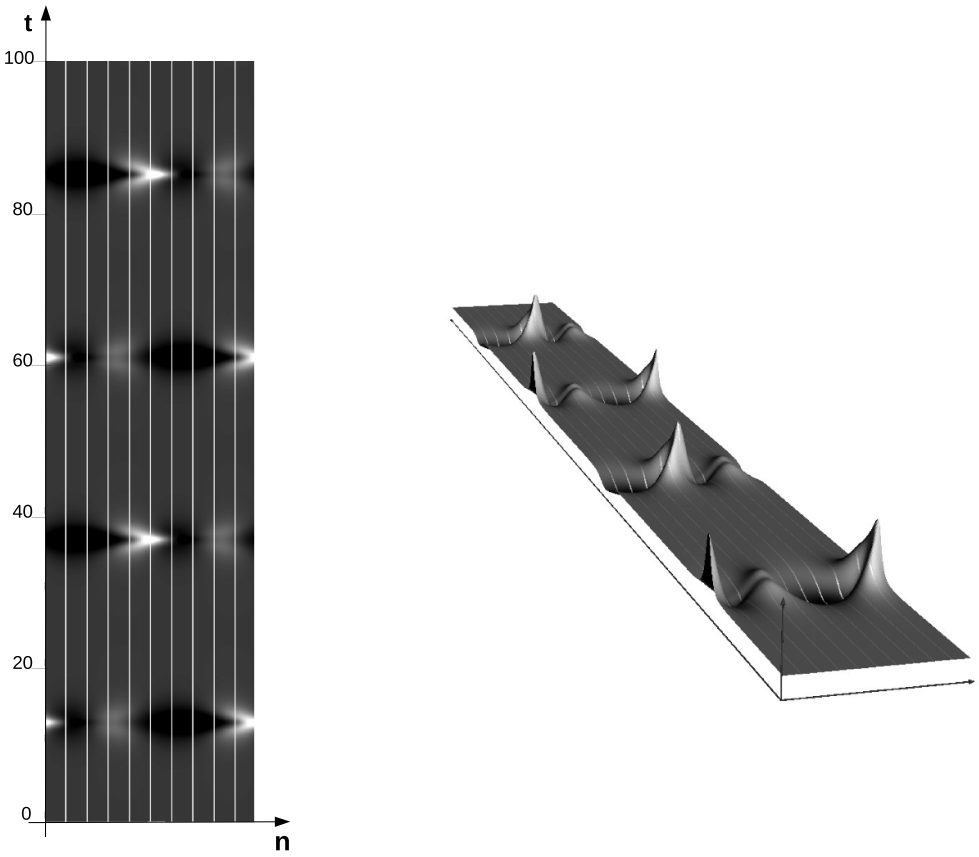

Figure 8. Density and 3D plots of $|u(n,t)|$, with two unstable modes, with $N=10$, $a=0.8$ and $\epsilon=10^{-5}$. The numerical integration is performed using the 6th order Runge-Kutta. The initial condition is $u_n(0)=a(1+\epsilon(c_1e^{i\kappa_1 n}+c_{-1}e^{-i\kappa_1 n}+c_2e^{i\kappa_2 n}+c_{-2}e^{-i\kappa_2 n}))$, where $\kappa_1=\frac{2\pi}{N}$, $\kappa_2=2\kappa_1$, $c_1=-0.2541+i\ 0.6967$, $c_{-1}=-0.3492+i\,0.6642$, $c_2=1.016+i\,16.87$, $c_{-2}=-6.402-i\,15.19$, and $\epsilon=10^{-5}$. The coefficients $c_{\pm j}$ are chosen to have $|t_1^{(j)}-t_2^{(j)}|\ll 1$, $j=0,1$; these two conditions imply that the two unstable modes appear approximately at the same time for many recurrences.

$$u_n(t)=a\,e^{-2i|a|^2t}\Bigg\{1-\epsilon\sum_{j=1}^{p}\Bigg[\frac{|\alpha_j|}{\sin(2\phi_j)}e^{\sigma_j t-i\phi_j}\cos\left(\kappa_j\left(n-X_j^+\right)\right)+\frac{|\beta_j|}{\sin(2\phi_j)}e^{-\sigma_j t+i\phi_j}\cos\left(\kappa_j\left(n-X_j^-\right)\right)\Bigg]+O\left(\epsilon^2\right),\tag{78}$$

where σ_j, ϕ_j, $X_j^{\pm}$, α_j, β_j, $1\leqslant j\leqslant p$ are defined respectively in (51), (52) and (53).

This solution grows exponentially and generically develops singularities of the type discussed in section 3 in the first nonlinear stage, when $t=O(\log(1/\epsilon))$. Therefore it does no make sense to study its recurrence properties, but it does make sense to see how a smooth initial condition (48) evolves into a singularity in finite time.

If $p=1$, then the period is $N=3$, and κ_1 is the only unstable mode. The matching procedure of the previous section leads to the comparison between the linearized solution (78) and the one mode solution (figure 3) in the intermediate region $O(1) \ll t \ll \sigma_1^{-1}\log(|\epsilon|)$:

$$\begin{aligned} &u \sim a e^{-2i|a|^2 t}\left[1-\epsilon\tfrac{|\alpha_1|}{\sin(2\phi_1)}e^{\sigma_1 t - i\phi_1}\cos\left[\kappa_1\left(x-X_1^+\right)\right]\right], \\ &\mathcal{N}_1 \sim a e^{-2i|a|^2 t} e^{i(\rho+2\phi_1)}\left[1-\epsilon\tfrac{4G_1\cos\theta_1}{\gamma^+}e^{\Sigma_1(t-T_1)-i\theta_1}\cos\left[K_1\left(x-X_1\right)\right]\right], \\ &T_1 = \tfrac{1}{\sigma_1}\log\left(\tfrac{\gamma^+}{\epsilon}\right), \end{aligned} \tag{79}$$

inferring that $\rho=-2\phi_1$, $\kappa=\kappa_1$ (consequently $\theta_1=\phi_1$ and $\Sigma_1=\sigma_1$), $X_1=X_1^+$, and

$$\gamma^+ = \frac{2\sin^2(2\phi_1)}{|\alpha_1|\cos(\kappa_1/2)} \quad \Rightarrow \quad T_1 = t^{(1)} := \frac{1}{\sigma_1}\log\left(\frac{\sigma_1^2}{2\epsilon|a|^4|\alpha_1|\cos(\kappa_1/2)}\right). \tag{80}$$

Therefore the smooth initial condition $u_n(0)=a\left[1+\epsilon\left(c_1 e^{i\kappa_1 n}+c_{-1}e^{-i\kappa_1 n}\right)\right]$ evolves into the generically singular solution

$$u_n(t) \sim \mathcal{N}_1\left(n,t;\kappa_1,X_1^+,t^{(1)},-2\phi_1,-1\right), \quad |t-t^{(1)}| = O(1), \tag{81}$$

whose singularity properties have been studied in section 3. Analogously, in the case $p=2$, corresponding to the two unstable modes κ_j, $j=1,2$ and to the period $N=5$, the smooth initial condition

$$u_n(0) = a\left[1+\epsilon\sum_{j=1}^{2}\left(c_j e^{i\kappa_j n}+c_{-j}e^{-i\kappa_j n}\right)\right] \tag{82}$$

evolves into the generically singular two-breather solution

$$u_n(t) \sim \mathcal{N}_2\left(n,t;\kappa_1,\kappa_2,X_1^+,X_2^+,t_1^{(1)},t_2^{(1)},-2(\phi_1+\phi_2),-1\right), \tag{83}$$

where $X_1^+, X_2^+, t_1^{(1)}, t_2^{(1)}$ are the same as in the $\eta=1$ case, shown in (76) (see figure 6).

5. Conclusions and future perspectives

In this paper we have first introduced known and new periodic exact AW solutions of the AL equations, using classical DTs, and we have established their relevance in the description of the AW dynamics for generic periodic initial perturbations of the background, in the case of one and two unstable modes only, using matched asymptotic expansions, in excellent agreement with numerical simulations. If $\eta=1$ the solution describes a FPUT recurrence of regular AWs, while in the case $\eta=-1$ and for a sufficiently large background, the solution describes, through elementary functions, how a generic regular periodic initial perturbation of the background evolves into a blow-up at finite time. This last regime cannot be captured by the defocusing NLS equation, and the proper continuous limit describing it is also performed, leading to NLS equations with a nonlinear and weak dispersion, from which it is transparent that the case in which $\eta=-1$ and the amplitudes are sufficiently large describes a strongly focusing regime. These results open several research directions. First, the FG method for AWs, partially developed in [20], should be suitably implemented to study the periodic AL Cauchy problem of AWs in the case of an arbitrary finite number of unstable modes, when matched asymptotics are not an adeguate tool since asymptotic regions are not well separated. Second, the perturbation theory of AWs of the AL equations, developed in [20], should allow one to study the dynamics of AWs of non integrable but physically relevant lattice NLS equations close

to the AL lattices. Third, since the NLS equations with nonlinear and weak dispersion (46) are quasi integrable, since they possess an approximate Lax pair [17], the corresponding IST and FG methods should be developed; in addition the study of possible applications of these equations should also be done. At last, a natural generalization of the results of this paper consists in studying the AW dynamics of periodic AWs of vector/matrix generalizations of the AL equations [6] (see [21, 22] for some studies of AWs for vector generalizations of NLS).

Data availability statement

All data that support the findings of this study are included within the article (and any supplementary files).

Acknowledgments

This research was supported by the Research Project of National Interest (PRIN) No. 2020X4T57A. It was also done within the activities of the INDAM-GNFM.

Appendix. Darboux transformations and periodic AW solutions

We look for a gauge transformation matrix $D_n(t,\lambda)$ (the so-called Darboux matrix) that preserves the structure and the symmetries of the AL Lax pair. More precisely, let $(u_n^{[0]},\vec{\psi}_n^{[0]})$ and $(u_n,\vec{\psi}_n)$ be solutions of the Lax pair (4). Then we look for the transformation

$$\vec{\psi}_n = D_n(t,\lambda)\,\vec{\psi}_n^{[0]}, \tag{84}$$

implying the following two equations for the Darboux matrix

$$D_{n+1}L_n^{[0]} = L_n D_n, \quad D_{n_t} = A_n D_n - D_n A_n^{[0]}, \tag{85}$$

where $(L_n^{[0]},A_n^{[0]})$ are the matrices (L_n,A_n) in (4) in which u_n is replaced by $u_n^{[0]}$, together with the symmetry

$$D_n(\lambda) = P_\eta\,\overline{D_n\left(\frac{1}{\bar{\lambda}}\right)}\,P_\eta^\dagger \tag{86}$$

coming from (5) and (6).

Following [27], we look for the Darboux matrix in the form:

$$D_n(\lambda) = \begin{pmatrix} \lambda^K + \sum_{l=1}^{N} a_n^{(K-2l)}\lambda^{K-2l} & \sum_{l=1}^{K} b_n^{(K-2l+1)}\lambda^{K-2l+1} \\ \sum_{l=1}^{K} c_n^{(K-2l+1)}\lambda^{-K+2l-1} & \lambda^{-K} + \sum_{l=1}^{K} d_n^{(K-2l)}\lambda^{-K+2l} \end{pmatrix}, \tag{87}$$

for $K\in\mathbb{N}^+$, corresponding to the Darboux transformation

$$\vec{\psi}_n^{[K]} = D_n(t,\lambda)\,\vec{\psi}_n^{[0]}; \tag{88}$$

then the symmetry (86) implies the following relations between the matrix elements of $D_n^{(K)}$:

$$d_n^{(l)} = \overline{a_n^{(l)}}, \quad c_n^{(l)} = -\eta \overline{b_n^{(l)}}. \tag{89}$$

It is well-known that the Darboux matrix describes a one-parameter (the complex parameter λ) family of transformations becoming singular at one or more values of λ. If λ_i is a singular point such that $\det D_n(\lambda_i, t) = 0$, the symmetries of the Lax pair imply that also $-\lambda_i$ and $\pm 1/\overline{\lambda}_i$ are singular points. At the singular points $(\pm\lambda_i, \pm 1/\overline{\lambda}_i)$ the matrix $D_n(\lambda, t)$ has range 1 and, if $\underline{\xi}_n(t,\lambda), \underline{\chi}_n(t,\lambda)$ are the columns of the fundamental matrix solution $\Psi_n^{[0]}(t,\lambda)$ of the Lax pair (4) for $u_n = u_n^{[0]}$: $\Psi_n^{[0]}(t,\lambda) = \left(\underline{\xi}_n(t,\lambda), \underline{\chi}_n(t,\lambda)\right)$, their images must be proportional in the points $(\pm\lambda_i, \pm 1/\overline{\lambda_i})$ where the matrix is singular:

$$D_n(\lambda_i) \cdot \left(\underline{\xi}_n(\lambda_i) - \gamma_i \underline{\chi}_n(\lambda_i)\right) = \underline{0}, \tag{90}$$

where γ_i is the proportionality factor.

Equation (90) implies, for each λ_i, the system:

$$\begin{aligned} &\left(\lambda_i^K + \sum_{l=1}^{K} a_n^{(K-2l)} \lambda_i^{K-2l}\right) + \left(\sum_{l=1}^{K} b_n^{(K-2l+1)} \lambda_i^{K-2l+1}\right) r_i = 0, \\ &\left(\frac{1}{\overline{\lambda}_i^K} + \sum_{l=1}^{K} \frac{a_n^{(K-2l)}}{\overline{\lambda}_i^{K-2l}}\right) - \eta \left(\sum_{l=1}^{K} \frac{b_n^{(K-2l+1)}}{\overline{\lambda}_i^{K-2l+1}}\right) \frac{1}{\overline{r_i}} = 0, \end{aligned} \tag{91}$$

where

$$r_i = \frac{(\xi_n(\lambda_i))_2 - \gamma_i \, (\chi_n(\lambda_i))_2}{(\xi_n(\lambda_i))_1 - \gamma_i \, (\chi_n(\lambda_i))_1}. \tag{92}$$

Note that a change of the basis of the eigenvectors $\left(\underline{\xi}_n(t,\lambda), \underline{\chi}_n(t,\lambda)\right)$ is equivalent to a rescaling of the constant γ_i. If the number of singular points λ_i is equal to the order K of the Darboux transformation, the relations (91) for $i = 1, \dots, K$ define a determined system of $2K$ equations for the $2K$ unknowns $a_n^{(l)}$, $b_n^{(l)}$, $l = 1, \dots, K$, that can be uniquely solved, leading to the wanted Darboux matrix.

At last, from the first of equation (85), the dressed solution $u_n^{[K]}(t)$ can be calculated from the solution $u_n^{[0]}(t)$ in the following way:

$$u_n^{[K]}(t) = u_n^{[0]}(t) \, a_{n+1}^{(-K)}(t) + b_{n+1}^{(-K+1)}(t). \tag{93}$$

Now we specialize the previous formulas for the two simplest cases $K = 1, 2$.

$K = 1$

If $K = 1$, the linear system (91) of two equations yields the solution

$$\begin{aligned} a_n^{(-1)}(t) &= \frac{\Delta_a^{(1)}}{\Delta^{(1)}} = -\frac{\eta\lambda_1 + \dfrac{|r_1|^2}{\overline{\lambda_1}}}{|r_1|^2 \overline{\lambda_1} + \frac{\eta}{\lambda_1}}, \\ b_n^{(0)}(t) &= \frac{\Delta_b^{(1)}}{\Delta^{(1)}} = -\frac{\overline{r_1}}{|r_1|^2 \overline{\lambda_1} + \frac{\eta}{\lambda_1}} \left(|\lambda_1|^2 - \frac{1}{|\lambda_1|^2}\right), \end{aligned} \tag{94}$$

where

$$\Delta_a^{(1)} = \det \begin{pmatrix} -\lambda_1 & r_1 \\ -\frac{1}{\overline{\lambda_1}} & -\frac{\eta}{\overline{r_1}} \end{pmatrix}, \quad \Delta_b^{(1)} = \det \begin{pmatrix} \frac{1}{\lambda_1} & -\lambda_1 \\ \overline{\lambda_1} & -\frac{1}{\overline{\lambda_1}} \end{pmatrix}, \quad \Delta^{(1)} = \det \begin{pmatrix} \frac{1}{\lambda_1} & r_1 \\ \overline{\lambda_1} & -\frac{\eta}{\overline{r_1}} \end{pmatrix}.$$

At last:

$$u_n^{[1]}(t) = u_n^{[0]}(t)\, a_{n+1}^{(-1)}(t) + b_{n+1}^{(0)}(t). \tag{95}$$

$K = 2$

If $K = 2$, we can write the relevant Darboux matrix elements $a_n^{(-2)}$ and $b_n^{(1)}$ through the formulas:

$$a_n^{(-2)}(t) = \frac{\Delta_a^{(2)}}{\Delta^{(2)}}, \qquad b_n^{(-1)}(t) = \frac{\Delta_b^{(2)}}{\Delta^{(2)}}, \tag{96}$$

where

$$\Delta^{(2)} = \det \begin{pmatrix} 1 & \frac{1}{\lambda_1^2} & r_1\lambda_1 & \frac{r_1}{\lambda_1} \\ 1 & \frac{1}{\lambda_2^2} & r_2\lambda_2 & \frac{r_2}{\lambda_2} \\ 1 & \overline{\lambda_1}^2 & -\frac{\eta}{\overline{\lambda}_1\overline{r_1}} & -\frac{\eta\overline{\lambda}_1}{\overline{r_1}} \\ 1 & \overline{\lambda_2}^2 & -\frac{\eta}{\overline{\lambda}_2\overline{r_2}} & -\frac{\eta\overline{\lambda}_2}{\overline{r_2}} \end{pmatrix},$$

and $\Delta_a^{(2)}$ and $\Delta_b^{(2)}$ are obtained substituting in $\Delta^{(2)}$ the second and the fourth columns, respectively, by the vector $(-\lambda_1^2, -\lambda_2^2, -1/\overline{\lambda_1}^2, -1/\overline{\lambda_2}^2)^T$. As for the previous case, specializing (93) for $K = 2$, we obtain the solution:

$$u_n^{[2]}(t) = u_n^{[0]}(t)\, a_{n+1}^{(-2)}(t) + b_{n+1}^{(-1)}(t). \tag{97}$$

The Darboux dressing of the background solution

Now we specialize this construction choosing $u_n^{[0]}(t) = a\, e^{2i\eta|a|^2 t}$ (the background solution); then the matrix fundamental solution of the Lax pair reads:

$$\begin{aligned} \Psi_n^{[0]}(\lambda;t) &= \left(\underline{\xi}_n(t,\lambda), \underline{\chi}_n(t,\lambda)\right) \\ &= \left(1+\eta|a|^2\right)^{\frac{n}{2}} e^{i\left(|a|^2 t + \frac{\arg a}{2}\right)\sigma_3} \begin{pmatrix} e^{i\frac{\eta}{2}(kn-\phi)-\frac{\sigma t}{2}} & -e^{-i\frac{\eta}{2}(kn-\phi)+\frac{\sigma t}{2}} \\ \frac{i}{\sqrt{\eta}} e^{i\frac{\eta}{2}(kn+\phi)-\frac{\sigma t}{2}} & \frac{i}{\sqrt{\eta}} e^{-i\frac{\eta}{2}(kn+\phi)+\frac{\sigma t}{2}} \end{pmatrix} e^{i\nu t}, \end{aligned} \tag{98}$$

where

$$\begin{aligned} &\cos\left(\tfrac{k}{2}\right) = \tfrac{\left(\lambda+\lambda^{-1}\right)}{2\sqrt{1+\eta|a|^2}} \;\Leftrightarrow\; \lambda = \sqrt{1+\eta|a|^2}\cos(\kappa/2) + |a|\sqrt{\eta}\sin\phi, \\ &\cos\phi = \sqrt{1+\tfrac{\eta}{|a|^2}}\sin\left(\tfrac{k}{2}\right), \\ &\nu = 2|a|\sqrt{\eta+|a|^2}\sin\phi\cos\tfrac{k}{2}. \end{aligned} \tag{99}$$

Therefore the building blocks of the solutions (95) and (97), are the functions $r_i(n,t)$, calculated from (98) and (92) in the following form:

$$r_i = -\sqrt{\eta}\,\frac{\sin\left(\dfrac{\kappa_i\,(n-n_i)+i\eta\sigma_i\,(t-t_i)+\phi_i}{2}\right)}{\cos\left(\dfrac{\kappa_i\,(n-n_i)+i\eta\sigma_i\,(t-t_i)-\phi_i}{2}\right)}\,e^{-2i\eta|a|^2t-i\arg a}, \tag{100}$$

where $n_i = \eta\frac{\arg\gamma_i}{\kappa_i}$ and $t_i = -\frac{log(|\gamma_i|)}{\sigma_i}$, and the singularities λ_i are expressed in terms of the modes κ_i and the angles ϕ_i via (99):

$$\lambda_i = \sqrt{1+\eta|a|^2}\cos(\kappa_i/2) + |a|\sqrt{\eta}\sin\phi_i. \tag{101}$$

Substituting (100) and (101) into equations (94) and (96) we construct the relevant coefficients of the Darboux matrices under construction; then formulas (95) and (97) give the wanted solutions, equivalent to the one and two breather solutions (24) and (38), through the following relations among the parameters.

For the one mode solution $\mathcal{N}_1(n,t;K_1,X_1,T_1,\rho,\eta)$ in (24): $K_1=\kappa_1$, $\theta_1=\phi_1$, $X_1 = n_1 - \frac{\eta}{2} - \frac{\pi}{2K_1}$, $T_1 = t_1$, and $\rho=\pi$.

For the two mode solution $\mathcal{N}_2(n,t;K_1,K_2,X_1,X_2,T_1,T_2,\rho,\eta)$ in (38): $K_j=\kappa_j$, $\theta_j=\phi_j$, $X_1 = n_1 - \frac{1}{2} - \frac{\pi}{2K_1}$, $X_2 = n_2 - \frac{1}{2} + \frac{\pi}{2K_2}$, $T_j = t_j$, $\rho=0$, $j=1,2$.

ORCID iDs

F Coppini https://orcid.org/0000-0001-9992-5457
P M Santini https://orcid.org/0000-0003-0722-9505

References

[1] Ablowitz M J, Biondini G and Prinari B 2007 Inverse scattering transform for the integrable discrete nonlinear Schrödinger equation with non-vanishing boundary conditions *Inverse Problems* **23** 1711–58
[2] Ablowitz M J and Ladik J F 1975 Nonlinear differential-difference equations *J. Math. Phys.* **16** 598–603
[3] Ablowitz M J and Ladik J F 1976 Nonlinear differential-difference equations and Fourier analysis *J. Math. Phys.* **17** 1011–8
[4] Ablowitz M J and Musslimani Z H 2013 Integrable nonlocal nonlinear Schrödinger equation *Phys. Rev. Lett.* **110** 064105
[5] Ablowitz M J and Segur H 1981 *Solitons and the Inverse Scattering Transform* (SIAM)
[6] Ablowitz M, Prinari B and Trubatch A 2003 *Discrete and Continuous Nonlinear SchröDinger Systems* (*London Mathematical Society Lecture Note Series*) (Cambridge University Press)
[7] Akhmediev N and Ankiewicz A 2011 Modulation instability, '-Pasta-Ulam recurrence, rogue waves, nonlinear phase shift and exact solutions of the Ablowitz-Ladik equation *Phys. Rev.* E **83** 046603
[8] Akhmediev N N, Eleonskii V M and Kulagin N E 1985 Generation of periodic trains of picosecond pulses in an optical fiber: exact solutions *Sov. Phys. - JETP* **62** 894–9
[9] Benjamin T B and Feir J E 1967 The disintegration of wave trains on deep water. Part I. Theory *J. Fluid Mech.* **27** 417–30
[10] Bespalov V I and Talanov V I 1966 Filamentary structure of light beams in nonlinear liquids *JETP Lett.* **3** 307–10
[11] Biondini G and Kovacic G 2014 Inverse scattering transform for the focusing nonlinear Schrödinger equation with nonzero boundary conditions *J. Math. Phys.* **55** 031506
[12] Biondini G, Li S and Mantzavinos D 2016 Oscillation structure of localized perturbations in modulationally unstable media *Phys. Rev.* E **94** 060201(R)

[13] Biondini G, Li S, Mantzavinos D and Trillo S 2018 Universal behavior of modulationally unstable media *SIAM Rev.* **60** 888–908
[14] Chubykalo O A, Konotop V V, Vazquez L and Vekslerchik V E 1992 Some features of the repulsive discrete nonlinear Schrödinger equation *Phys. Lett.* A **169** 359–63
[15] Coppini F, Grinevich P G and Santini P M 2020 The effect of a small loss or gain in the periodic NLS anomalous wave dynamics. I *Phys. Rev.* E **101** 032204
[16] Coppini F, Grinevich P G and Santini P M 2022 Periodic rogue waves and perturbation theory *Encyclopedia of Complexity and Systems Science* ed R A Meyers (Springer)
[17] Coppini F and Santini P M Quasi integrable NLS equations with a nonlinear and weak dispersion *Preprint* (in preparation)
[18] Coppini F and Santini P M 2020 The Fermi-Pasta-Ulam-Tsingou recurrence of periodic anomalous waves in the complex Ginzburg-Landau and in the Lugiato-Lefever equations *Phys. Rev.* E **102** 062207
[19] Coppini F and Santini P M 2023 The massive thirring model: exact solutions and Fermi-Pasta-Ulam-Tsingou recurrence of anomalous waves *Preprint* (in preparation)
[20] Coppini F and Santini P M The effect of loss/gain and Hamiltonian perturbations of the Ablowitz-Ladik lattice on the recurrence of periodic anomalous waves (arXiv:2305.07339)
[21] Degasperis A, Lombardo S and Sommacal M 2017 Integrability and linear stability of nonlinear waves *J. Nonlinear Sci.* **28** 1251–91
[22] Degasperis A, Lombardo S and Sommacal M 2019 Rogue wave type solutions and spectra of coupled nonlinear Schrödinger equations *Fluids* **4** 57
[23] Doliwa A and Santini P M 1995 Integrable dynamics of a discrete curve and the Ablowitz-Ladik hierarchy *J. Math. Phys.* **36** 1259–73
[24] Dubrovin B A 1975 Inverse problem for periodic finite-zoned potentials in the theory of scattering *Funct. Anal. Appl.* **9** 61–62
[25] Dysthe K B and Trulsen K 1999 Note on breather type solutions of the NLS as models for freak-waves *Phys. Scr.* **T82** 48–52
[26] Gallavotti G (ed) 2008 *The Fermi-Pasta-Ulam Problem: A Status Report* (*Lecture Notes in Physics* vol 728) (Springer)
[27] Geng X 1989 Darboux transformation of the discrete Ablowitz-Ladik eigenvalue problem *Acta Math. Sci.* **9** 21–26
[28] Grinevich P G and Santini P M 2018 The finite gap method and the analytic description of the exact rogue wave recurrence in the periodic NLS Cauchy problem. 1 *Nonlinearity* **31** 5258–308
[29] Grinevich P G and Santini P M 2018 Phase resonances of the NLS rogue wave recurrence in the quasi-symmetric case *Theor. Math. Phys.* **196** 1294–306
[30] Grinevich P G and Santini P M 2018 The exact rogue wave recurrence in the NLS periodic setting via matched asymptotic expansions, for 1 and 2 unstable modes *Phys. Lett.* A **382** 973–9
[31] Grinevich P G and Santini P M 2019 The finite-gap method and the periodic NLS Cauchy problem of anomalous waves for a finite number of unstable modes *Russ. Math. Surv.* **74** 211–63
[32] Grinevich P G and Santini P M 2021 The linear and nonlinear instability of the Akhmediev breather *Nonlinearity* **34** 8331–58
[33] Grinevich P G and Santini P M 2018 Numerical instability of the Akhmediev breather and a finite-gap model of it *Recent Developments in Integrable Systems and Related Topics of Mathematical Physics* (*MP 2016*) (*Springer Proceedings in Mathematics and Statistics* vol 273) ed V Buchstaber, S Konstantinou-Rizos and A Mikhailov (Springer)
[34] Henderson K L, Peregrine D H and Dold J W 1999 Unsteady water wave modulations: fully nonlinear solutions and comparison with the nonlinear Schrödinger equation *Wave Motion* **29** 341–61
[35] Hirota R 1971 *Phys. Rev. Lett.* **27** 1192
[36] Infeld E 1981 Quantitive theory of the Fermi-Pasta-Ulam recurrence in the nonlinear Schrödinger equation *Phys. Rev. Lett.* **47** 717–8
[37] Ishimori Y 1982 An integrable classical spin chain *J. Phys. Soc. Japan* **51** 3417–8
[38] Its A R, Izergin A G, Korepin V E and Slavnov N A 1991 Temperature correlations of quantum spins *Phys. Rev. Lett.* **70** 1704–6
[39] Its A R and Kotljarov V P 1976 Explicit formulas for solutions of a nonlinear Schrödinger equation *Dokl. Akad. Nauk Ukrain. SSR Ser.* A **1051** 965–8
[40] Its A R and Matveev V B 1975 Hill's operator with finitely many gaps *Funct. Anal. Appl.* **9** 65–66
[41] Its A R, Rybin A V and Sall M A 1988 Exact integration of nonlinear Schrödinger equation *Theor. Math. Phys.* **74** 20–32

[42] Kharif C and Pelinovsky E 2004 Physical mechanisms of the rogue wave phenomenon *Eur. J. Mech.* B **22** 603–34
[43] Kharif C, Pelinovsky E, Talipova T and Slunyaev A 2011 Focusing of nonlinear wave groups in deep water *JETP Lett.* **73** 170–5
[44] Kimmoun O *et al* 2016 Modulation instability and phase-shifted Fermi-Pasta-Ulam recurrence *Sci. Rep.* **6** 28516
[45] Krichever I M The periodic non-Abelian Toda chain and its two-dimensional generalization; Appendix of [24]
[46] Krichever I M 1977 Methods of algebraic Geometry in the theory on nonlinear equations *Russ. Math. Surv.* **32** 185–213
[47] Kuznetsov E A 1977 Solitons in a parametrically unstable plasma *Sov. Phys. Dokl.* **22** 507–8
[48] Lieb E, Schultz T and Mattis D 1961 Two soluble models of an antiferromagnetic chain *Ann. Phys., NY* **16** 407–46
[49] Lugiato L A and Lefevre R 1987 Spatial dissipative structures in passive optical systems *Phys. Rev. Lett.* **85** 2209–11
[50] Ma Y C 1979 The perturbed plane wave solutions of the cubic Schrödinger equation *Stud. Appl. Math.* **60** 43–58
[51] Marquié P, Bilbault J M and Remoissenet M 1995 Observation of nonlinear localized modes in an electrical lattice *Phys. Rev.* E **51** 6127–33
[52] Mikhailov A V 1976 Integrability of the two-dimensional Thirring model *JETP Lett. USSR* **23** 6 (Engl. Transl.)
[53] Miller P D, Ercolani N M, Krichever I M and Levermore C D 1995 Finite genus solutions to the Ablowitz–Ladik equations *Commun. Pure Appl. Math.* **48** 1369–440
[54] Mussot A, Naveau C, Conforti M, Kudlinski A, Szriftgiser P, Copie F and Trillo S 2018 Fibre multiwave-mixing combs reveal the broken symmetry of Fermi-Pasta-Ulam recurrence *Nat. Photon.* **12** 303–8
[55] Narita K 1991 Soliton solutions for discrete Hirota equation II *J. Phys. Soc. Japan* **60** 1497–500
[56] Newell A C and Whitehead J A 1969 Review of the finite bandwidth concept *Proc. IUTAM* (*Symp. on Instability of Continuous Systems*) (Springer) pp 284–9
[57] Novikov S P 1974 The periodic problem for the Korteweg-de Vries equation *Funct. Anal. Appl.* **8** 236–46
[58] Ohta Y and Yang J 2014 General rogue waves in the focusing and defocusing Ablowitz-Ladik equations *J. Phys. A: Math. Theor.* **47** 255201
[59] Onorato M, Residori S, Bortolozzo U, Montina A and Arecchi F T 2013 Rogue waves and their generating mechanisms in different physical contexts *Phys. Rep.* **528** 47–89
[60] Ortiz A K and Prinari B 2019 Inverse scattering transform for the defocusing Ablowitz-Ladik equation with arbitrarily large background *Stud. App. Math.* **143** 337–448
[61] Osborne A, Onorato M and Serio M 2000 The nonlinear dynamics of rogue waves and holes in deep-water gravity wave trains *Phys. Lett.* A **275** 386–93
[62] Peregrine D H 1983 Water waves, nonlinear Schrödinger equations and their solutions *ANZIAM J.* B **25** 16–43
[63] Pierangeli D, Flammini M, Zhang L, Marcucci G, Agranat A J, Grinevich P G, Santini P M, Conti C and DelRe E 2019 Observation of exact Fermi-Pasta-Ulam-Tsingou recurrence and its exact dynamics *Phys. Rev.* X **8** 041017
[64] Prinari B 2016 Discrete solitons of the focusing Ablowitz-Ladik equation with nonzero boundary conditions via inverse scattering *J. Math. Phys.* **57** 083510
[65] Prinari B and Vitale F 2016 Inverse scattering transform for the focusing Ablowitz-Ladik system with nonzero boundary conditions *Stud. Appl. Math.* **137** 28–52
[66] Santini P M 2018 The periodic Cauchy problem for PT-symmetric NLS, I: the first appearance of rogue waves, regular behavior or blow up at finite times *J. Phys. A: Math. Theor.* **51** 495207
[67] Sarafyan D 1972 Improved sixth-order Runge-Kutta formulas and approximate continuous solution of ordinary differential equations *J. Math. Anal. Appl.* **40** 436–45
[68] Schober C M 1991 Numerical and analytical studies of the discrete nonlinear Schroedinger equation *PhD Thesis* University of Arizona
[69] Soto-Crespo J M, Devine N and Akhmediev N 2017 Adiabatic transformation of continuous waves into trains of pulses *Phys. Rev.* A **96** 023825
[70] Stewart G 2023 Asymptotics for small data solutions of the Ablowitz-Ladik equation (arXiv:2303.10496)

[71] Takeno S and Hori K 1990 A propagating self-localized mode in a one-dimensional lattice with quartic anharmonicity *J. Phys. Soc. Japan* **59** 3037–40
[72] Thirring W E 1958 A soluble relativistic field theory *Ann. Phys., NY* **3** 91–112
[73] Trillo S and Wabnitz S 1991 Dynamics of the nonlinear modulational instability in optical fibers *Opt. Lett.* **16** 986–8
[74] Vekslerchik E and Konotop V V 1992 Discrete nonlinear Schrödinger equation under non-vanishing boundary conditions *Inverse Problems* **8** 889–909
[75] Yuen H C and Ferguson W E 1978 Relationship between Benjamin-Feir instability and recurrence in the nonlinear Schrödinger equation *Phys. Fluids* **21** 1275–8
[76] Yuen H and Lake B 1982 Nonlinear dynamics of deep-water gravity waves *Adv. Appl. Mech.* **22** 67–229
[77] Zakharov V E 1968 Stability of period waves of finite amplitude on surface of a deep fluid *J. Appl. Mech. Tech. Phys.* **9** 190–4
[78] Zakharov V E, Manakov S V, Noviko S P and Pitaevsky L P 1984 *Theory of Solitons* (Plenum)
[79] Zakharov V E and Shabat A B 1972 Exact theory of two-dimensional self-focusing and one-dimensional self-modulation of waves in nonlinear media *Sov. Phys - JETP* **34** 62–69
[80] Zakharov V and Ostrovsky L 2009 Modulation instability: the beginning *Physica* D **238** 540–8